Utrecht University

Master thesis Energy Science (2020-2021)

Optimization of Operation and Design of a Multi-Energy System for the Production of Low-Carbon Methanol

A case study for the industrial cluster of Rotterdam

Daan Bosma[1]

Supervised by Dr. Matteo Gazzani

Co-supervised by Jan Wiegner and Lukas Weimann

Second reader: Prof. Dr. Martin Junginger

[1]Date: 13-05-2021. Student No.: 5910765. Address: Amsterdamsestraatweg 117. Tel.: +31 6 348 682 63. Email: daan.bosma@hotmail.com.

Abstract

Methanol is one of the key feedstocks in the chemical industry and seen as a potential synthetic fuel replacement for maritime and air transport. Currently, most methanol is produced via the steam reforming of natural gas, resulting in significant greenhouse gas emissions. Sustainable methanol, on the other hand, can be produced via multiple pathways, each resulting in different energy and capital requirements, as well as CO_2 emissions.

This research integrates these different pathways in the context of a multi-energy system and linearly optimizes the design and operation of that system to analyse which pathway is preferred for the industrial cluster of Rotterdam in terms of associated costs and emissions per produced tonne of methanol. In this research, an assessment is made on the effect of (i) including and excluding a CO_2 storage facility, (ii) the type and origin of biomass and (iii) the steam biomass ratio in the biomass gasification routes on the optimal design of the multi-energy system.

It is found that the inclusion of a CO_2 storage facility significantly improves the optimal design of the multi-energy system in terms of both costs and emissions, making it even possible to obtain negative emissions with only minor cost increases. In this design, the preferred methanol production method is a biomass gasification method that includes CO_2 capture. Regarding the type of biomass it is found that biomass from close by is preferred due to lower costs and emissions associated with transport. Finally, a low steam biomass ratio is preferred; the lower biomass consumption at higher steam biomass ratios does weigh up against its higher steam consumption in terms of both costs and emissions.

Acknowledgements

First and foremost, I want to thank Matteo, Jan & Lukas for their continuous feedback and support during the process of conducting research for my thesis. Your guidance put me in the right direction and helped me in not only finalizing my thesis project, but also in doing better research overall. Extra appreciation goes to Jan for his help during the early, but also late, stages of modelling my research in the EHub tool; our meetings were always really fruitful.

Furthermore, I want to thank those that made sure that I sometimes took my mind off my thesis to relax a bit and enjoy life besides the thesis; at some stages during my thesis, I was dreaming of biomass steam gasification systems and realised I had to shift down a bit.

Grazie mille, Vielen Dank & Hartelijk dank to all persons involved during my thesis.

Contents

List of Tables

List of Figures

List of Abbreviations

BFB Bubbling Fluidized Bed

BtM Biomass-to-Methanol

CCU Carbon Capture & Utilisation

CCUS Carbon Capture & Utilisation + Storage

CFB Circulating Fluidized Bed

DAC Direct Air Capture

GHG Greenhouse Gas

KPI Key Performance Indicator

LHV Lower Heating Value

MeOH Methanol

MES Multi-Energy System

MILP Mixed-integer linear programming

PEMEC Proton Exchange Membrane Electrolyser

PEMFC Proton Exchange Membrane Fuel Cell

PWA Piecewise Affine (Approximation)

SBR Steam Biomass Ratio

WGS Water-Gas Shift

List of Mathematical Symbols

C_i	Installed capacity
$\widetilde{C_{i,m}}$	Auxiliary variable capacity
C_i^{max}	Maximum capacity
C_i^{min}	Minimum capacity
e	Emissions
J_c	Capital investment costs
J_o	Operational costs
J_m	Maintenance costs
L_t	Hourly load
$\widetilde{L_{t,m}}$	Auxiliary variable load
$p_{m,co2}$	KPI CO_2 production
$P_{t,MeOH}$	Hourly methanol production
S	Size of energy technology
u	Import price energy carrier
U	Power import energy carrier
v	Export price energy carrier
V	Power export energy carrier
x_m	Operational mode (SBR)
ϵ	Emission factor
$\epsilon_{m,el}$	KPI electricity
$\epsilon_{m,th}$	KPI heat
$\epsilon_{m,H2}$	KPI hydrogen
$\epsilon_{m,b}$	KPI biomass
λ	Variable cost coefficient
μ	Fixed variable cost coefficient
Ψ	Maintenance fraction
ω	annuity factor

1 Introduction

Societal Background

In December 2015, the Paris Agreement, a global agreement to mitigate climate change, was adopted. The proposed agreement aims at limiting global temperature rise to 1.5°C [62]. In order to comply with the Paris Agreement, the Dutch government adopted its own version, the Dutch Climate Agreement (Klimaatakkoord). One of the main contributors to these emissions and therewith one of the main candidates for decreasing greenhouse gas (GHG) emissions, is the industrial cluster of Rotterdam [51]. The industrial cluster of Rotterdam has already developed multiple decarbonization scenarios to decrease its emissions. These scenarios, however, only give a rough sketch on the potential future of the industrial cluster of Rotterdam and hence should be further researched [50]. In one of these potential decarbonization scenarios, the BIO-CCS scenario, there is a clear mention of the Rotterdam industrial cluster playing an important role in the production of synthetic fuels, such as methanol (MeOH), DME and Fischer-Tropsch fuels out of sustainable (biomass) resources. In this scenario, it is expected that future demand for fossil transport fuels (e.g. gasoline and diesel) goes down, while the demand for synthetic fuels increases. The inclusion of carbon capture and utilisation (CCU), potentially in combination with storage (CCUS), in that scenario is not left out as, according to Helseth et al., (2012) [29], biofuels production in combination with CCUS could result in negative emissions.

Especially the production of low-carbon methanol could have a significant impact on the decarbonization activities in the Rotterdam industrial cluster as it is not only a promising synthetic fuel, but also a widely used liquid in the (petro)chemical industry [5] [58]. Currently, most of the methanol is produced with natural gas as feedstock [14]. This natural gas is reformed with steam to produce synthesis gas (mixture of CO & H_2), which then reacts over a catalyst (usually a mixture of copper and zinc oxides) to produce methanol (ibid). Although this process is highly mature, it does use a significant amount of natural gas, leading to fossil fuel depletion and GHG emissions. Therefore, it is necessary to assess the feasibility of different production routes and technological configurations (e.g. in- and excluding CCU(S)) to produce low-carbon methanol. Therewith, this research aims to contribute to not only defining the feasibility of the different methods to produce low-carbon methanol, but also to better define the potential and technological characteristics related to the BIO-CCS scenario.

Scientific Background

In order to produce low-carbon methanol, two main routes exist. In the most mature of the two, methanol can be produced through the gasification of biomass to produce a synthesis gas. This synthesis gas must then be altered to be suitable for the methanol synthesis [48]. This can be done in two separate ways: first, it is possible to lower the carbon content through the removal (and potential compression and utilisation) of CO_2 with the use of carbon scrubbers, such as monoethanolamine (MEA) or Selexol [48]. Another possibility is to add compressed hydrogen to the gas mixture to increase the hydrogen content and assure the right synthesis gas composition [13] [66]. In a more novel route, low-carbon methanol can be produced through the process of combining compressed CO_2 and sustainable hydrogen. In this situation, a certain ratio of CO_2 and H_2 enters a synthesis reactor after which it is compressed into methanol [6]. Within both of these routes, there is either a demand or production of CO_2, making it worthwhile to also assess the feasibility of CCU or CCU+CCS (via the use of a carbon storage facility) to see if synergies between the two technologies can be achieved.

As these different production routes include multiple (energy) carriers (e.g. hydrogen, heat, electricity, CO_2), energy conversion technologies (e.g. electrolysers, biomass gasifiers) and potential synergies (e.g. the exchange CO_2), a multi-energy system (MES) approach would be suitable to research the potential of a system in which the routes are integrated. That is because a MES approach allows the different energy carriers to interact with each other on various levels (i.e. the so called Energy Hubs) [25]. This typically results in higher economic, technical and environmental performances than systems in which the operation and design of such energy systems takes place on a separate basis. This is due to the fact that the co-operation of the different energy carriers creates possibilities to increase overall efficiency, system reliability and load flexibility, while also taking into account potential synergies [25] [39]. In order to actually achieve a higher performance, an optimization of the MES is necessary. This optimization will provide insights in the appropriate sizing and operation schedules of the energy technologies, while making sure that demand is fulfilled. Currently, the mixed-integer linear programming (MILP) approach is the state of the art for the optimization of MES [64]. In the MILP approach, the processes concerning the different energy technologies and carriers in the MES are independently described via linear formulations and then reconstituted into an integrated system again. This can then be used to find the optimal design and operation of a MES, while making sure that computational time is not too long. [24] [23] [63].

Although optimization strategies, albeit for costs or emissions, for sustainable methanol production already exist, most of them focus on single parts in the methanol production process (e.g. the methanol synthesis or the biomass gasification), while typically not taking into account the total process or surrounding energy system [8]. Bozzano et al., (2016) [8] urges the need for a scientific trend towards the research of overall process and system optimization, as it would most likely result in reduced energy use and capital costs. As the biomass gasification routes carry a lot of dependencies related to both the amount and type of input (i.e. biomass, heat, electricity & hydrogen) and subsequent output (methanol), it is worthwhile to assess whether the operating parameters of the gasification process and the type of biomass have an impact on not only the methanol production, but also the optimal design and operation of the MES as a whole [54]. As such, this research aims to respond to the proposed urge from Bozzano et al., (2016).

In short, this research aims to focus on the multi-energy system approach for the production of low-carbon methanol at different configurations regarding the inclusion of a carbon storage facility, the type of biomass and the important operating parameters. The goal is to optimize the design and operation of a MES, as formulated by Geidl et al., (2007) [25], with the aid of MILP formulations, as defined in the Energy Hub tool by predominantly Gabrielli et al., (2018a), Gabrielli et al., (2018b), Gabrielli et al., (2019) & Weimann et al., (2020) [23] [65] [24] [22].

Research question(s)

To know how the optimal design and operation of a MES for the production of methanol looks like, the following main research question needs to be answered:

What is the optimal design and operation of a multi-energy system used for the production of methanol in the industrial cluster of Rotterdam in which costs are minimised for different emission constraints?

To answer this main research question, two different production systems are assessed. In both production systems, the type of biomass and the operating parameter of the steam biomass ratio in the biomass gasification process is altered to see which pathway is preferred in terms of minimizing the costs at different emission constraints. The operating parameter of the steam biomass ratio (the amount of steam used per kg of biomass input) is used, as according to Sreejith et al., (2012) [54], this parameter has a significant impact on the synthesis gas composition and hence the methanol output. For the type of biomass, three different types of biomass from different parts of the world are used as an input to the multi-energy system. An elaboration on the types of biomass and the steam biomass ratio is presented later in the methodology of this research.

The difference between the two production systems is that in one of the systems a carbon storage facility is available, while in the other system there is not. This is done to see how the inclusion or exclusion of a carbon storage facility impacts the overall system design and operation. The produced CO_2 in the context of this research therefore has three possible functionalities: it can either be used in other production processes, emitted into the air or, if applicable, stored underground.

This all leads to the following sub-questions:

What is the impact of using different types of biomass and different steam biomass ratios for the biomass gasification process on the optimal design and operation of a MES for the production of methanol and what is preferred for the industrial cluster of Rotterdam?

How does the in- or exclusion of a carbon storage facility impact the optimal design and operation of a MES for the production of methanol and what is preferred for the industrial cluster of Rotterdam?

By answering these research questions, this study contributes to the needs of the port of Rotterdam to decarbonize their activities by providing recommendations on how to design their future energy system for the production of methanol. Also, even though this study focuses on the case study of the industrial cluster of Rotterdam, the results can be used as a guideline for other ports or large industrial clusters that have, or aim to have, a high methanol production and want to reduce their carbon footprint. Besides, this research also builds upon the already existing Energy Hub tool by adding new technological components and carriers, such as the ones to be assessed in this research. This will not only broaden the knowledge and possibilities on optimizing the design and operation of multi-energy systems, but may also provide a solid tool for similar studies related to low-carbon methanol production.

The remainder of this thesis is as follows: first, a more detailed background on the system boundaries and methanol production technologies is presented. Next, the methodology on modelling the methanol production pathways and optimizing the MES is given. After that, results are shown and discussed and finally used to answer the posed research questions.

2 Technology & System description

This chapter is used to describe the main technologies that can be used to produce methanol. Also, an explanation is given on how these methanol production methods are contextualised in the larger picture of the multi-energy system approach.

2.1 Status quo in methanol production

Methanol is mostly produced by reforming natural gas with steam and then converting and distilling the resulting synthesis gas to create methanol [14]. Currently, the price of methanol is highly dependent on the price of natural gas, meaning that an increase in natural gas price ultimately leads to an increase in methanol price [35]. As of 2019, the methanol price in the Netherlands fluctuated between 250 and 400 EUR/tonne (325 EUR/tonne average) [35]. The emissions, associated with the production of methanol via the reforming of natural gas with steam, averaged around 0.7 tonnes of CO_2 per tonne of methanol [32]. This means that for methanol to be seen as 'low-carbon', emissions should at least be lower than 0.7 tonnes of CO_2 per tonne of methanol. The status quo in the production of methanol is not included in the multi-energy system approach. Rather, it is used to compare the outcomes of the more sustainable methods with the status quo.

2.2 Biomass gasification to produce methanol

Gasification process: In a more sustainable process, biomass is used as a feedstock for the production of methanol by gasifying it [13] [21] [66]. For the gasification process to be assessed in this research, a circulating fluidized bed (CFB) reactor is assumed, as this type of reactor fits best with large scale production of synthesis gas (used for methanol production), while also having a rather high flexibility regarding its load [41] [66] [53]. A bubbling fluidized bed (BFB) reactor is not assumed, as, according to Siedlecki et al., (2011) [53], it performs slightly worse than the CFB in terms of carbon conversion efficiency and tar production. Other types of biomass gasifiers include fixed bed and entrained flow reactors. The former is considered to be better for small scale production, while the latter can indeed be used for larger scale production of synthesis gas, but requires really fine powder as fuel input, leading to higher costs for the treatment of biomass (ibid). Regarding ramping rates and start up and shut down times, the following is assumed: a start up and shut down time of respectively 4 and 5 hours is assumed, based on the assumptions in Cali et al., (2020) [10]. For ramping rates it is assumed that 1 hour is sufficient to ramp between the different loads [34].

Besides biomass fuel, the gasification process requires a gasifying agent. This can be either pure oxygen, air, steam or a combination of those. In this research, steam is used as the gasifying agent as it results in both the highest hydrogen yield (which is preferred for methanol synthesis) and high tar and char reduction [44].

Gas cleaning and conditioning: After the gasification process, the synthesis gas (a mixture of CO, H_2 & CO_2) is separated from the ashes and waste gas products. The produced synthesis gas, however, typically has a too low hydrogen-to-carbon ratio (R) to make methanol (preferred ratio is between 2 and 2.1) [49]. This molar ratio is defined as follows:

$$R = \frac{H_2 + CO_2}{CO - CO_2} \tag{1}$$

In order to increase that ratio, the synthesis gas could be used as an input in a water-gas-shift reactor (WGSR) to increase the hydrogen content, after which it is moved to a carbon scrubber (requiring electricity) to remove CO_2. This CO_2 can then be either discarded or compressed for further utilisation or storage [66]. In another route, hydrogen (from water electrolysis) can be added to the synthesis gas in order to increase the hydrogen content. The former route is a cheaper and more matured method, while the latter route is more novel route that includes the addition of hydrogen. The main advantage there is the lower consumption of biomass, due to the fact that less hydrogen in the synthesis gas has to come from biomass. Therefore, both routes are used in the analysis to see which route is preferred.

$$3H_2 + CO_2 \rightleftharpoons CH_3OH + H_2O \tag{2}$$

$$2H_2 + CO \rightleftharpoons CH_3OH \tag{3}$$

Methanol synthesis: The outgoing, clean synthesis gas is compressed (requiring electricity), before it reacts over a catalyst (typically a mixture of copper and zinc oxides) to produce methanol via the reactions (2) and (3) shown above. Finally, this methanol is flashed to separate the pure methanol from the excess gases. This process is summarized in figure 1.

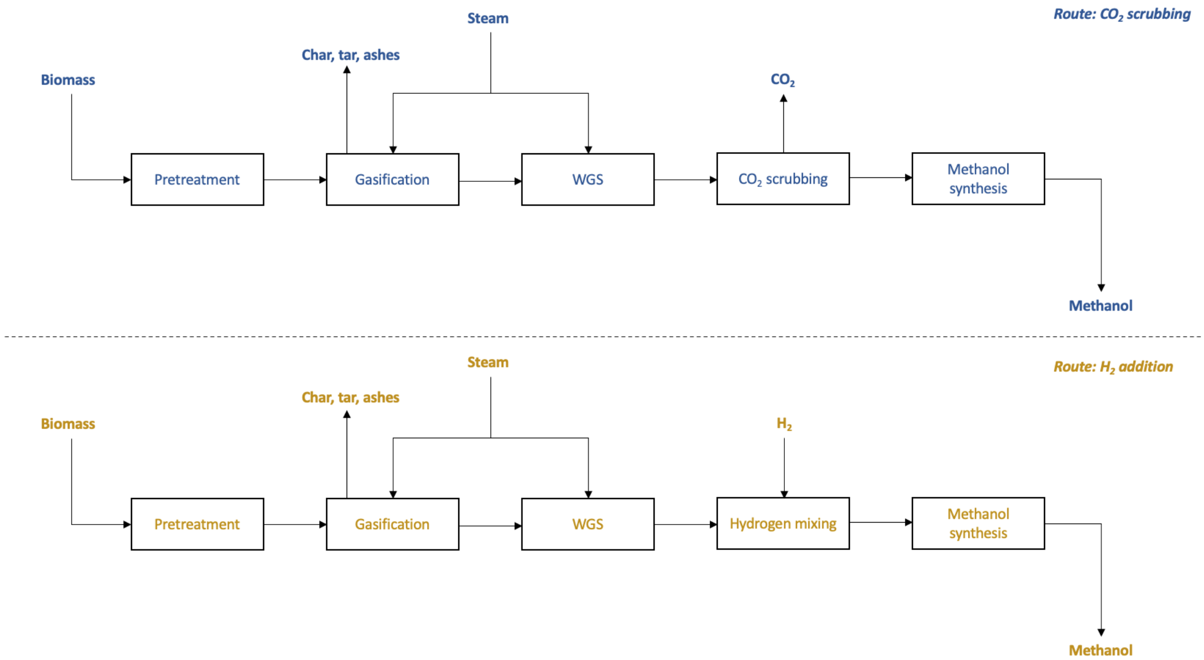

Figure 1: Methanol production process using biomass as feedstock with the route with respect to CO_2 removal and/or compression being displayed above and the route with respect to hydrogen addition being displayed below

2.3 CO_2 hydrogenation to produce methanol

A different method encompasses the hydrogenation of CO_2 with H_2. The CO_2 can either come from the biomass gasification process, where CO_2 is scrubbed from the synthesis gas mixture and compressed for further utilisation or it can come from a direct air capture (DAC) unit. In this unit, the CO_2 is captured in an air contactor through the process of absorption and subsequential desorption via a solid sorbent [6], which requires electricity and heat. After this, the pure stream of CO_2 is combined with H_2 (produced from water electrolysis). In this process, the H_2 and CO_2 combine through the process of hydrogenation to produce methanol.

$$3H_2 + CO_2 \rightleftharpoons CH_3OH + H_2O \tag{4}$$

In the end, the methanol is separated from the produced water to create a pure stream of methanol. This is summarized in the figure below.

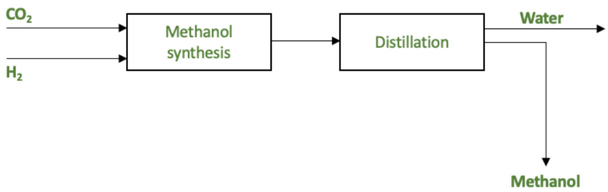

Figure 2: Methanol production from CO_2 and H_2

2.4 System description

To provide the energy inputs for either the biomass gasification, the following technologies are used within the boundaries of the energy system in this research.

Electricity can come from multiple sources. The energy system approach takes into account exported electricity, which comes at a certain price and emission factor. Electricity can also come from installed solar panels and on- or offshore wind turbines. There is also a possibility to store the electricity in Lithium-ion batteries for later use. **Heat** comes from boilers that run on either gas, electricity or hydrogen. Electric and hydrogen boilers are considered, as they are able to provide sustainable steam, while still being able to meet the temperature requirements for the steam (350°C, 1 bar) [54] [60] [61]. As the gasification process requires such high-temperature steam, heat cannot come from heat pumps due to their typical low-temperature nature. **Hydrogen**, needed for one of the gasification routes, the CO_2 hydrogenation and one of the boilers, comes from proton exchange membrame electrolysers (PEMEC). Hydrogen can also be stored in hydrogen storage tanks for later use or can be converted into electricity via a fuel cell (PEMFC). **CO_2** for the CO_2 hydrogenation process can be provided via either the biomass gasification plant following the CO_2 scrubbing and capture route or via the use of a direct-air capture (DAC) unit.

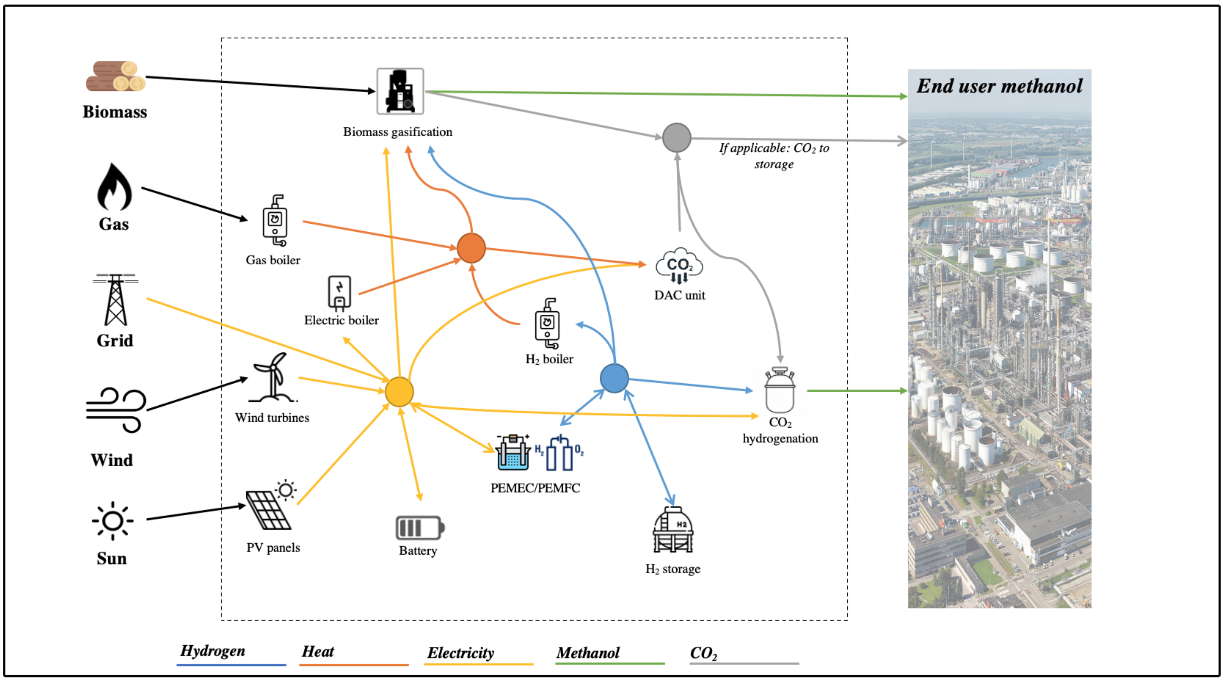

Figure 3: Multi-energy system visualization with the dotted line displaying the system boundaries. Offshore wind in this analysis is considered as an independent node providing electricity from the outside to this system

For all of these auxiliary technologies, linear formulations already exist in the EHub tool. Input data for these technologies (regarding performance and costs) is presented in the data collection section (section 3.3) of the methodology. The modelling approach for the different methods to produce methanol are also explained in the methodology, in section 3.2.

Based on this, the MES is visualized in Figure 3. The biomass gasification component in that figure encompasses three individual components. (i) the biomass gasification component in which CO_2 is scrubbed and emitted, (ii) the biomass gasification component in which CO_2 is scrubbed and captured for potential utilisation or storage (if applicable) and (iii) the biomass gasification component in which hydrogen is added to the synthesis gas mixture. Further explanation on the details of these components can be found in the methodology (section 3.2).

3 Methodology

In this section, the methodology for carrying out the proposed research is given. It starts with describing the main tool and assets to be used for formulating and solving the optimization problem regarding the optimal design of a MES for the production of methanol (section 3.1). After that, the modelling and implementation of the new components (i.e. the biomass gasification & CO_2 hydrogenation process) is explained (section 3.2). Finally, a description is given on the data collection and case studies to be assessed (section 3.3).

3.1 Methodology for solving MES optimization problems

3.1.1 EHub tool

The analysis is to be carried out in the Energy Hub (EHub) tool, as this tool allows for determining the optimal design of an energy system. The optimization is to be carried out over a time resolution of one year with input data, concerning weather, prices and emissions, coming from 2019. Uncertainties regarding future prices for biomass are assessed in a sensitivity analysis, which is elaborated on in section 3.3. To carry out the optimization of a MES, MATLAB is used as the programming language and Gurobi and YALMIP are used to solve the optimization problem [27]. The EHub tool is based on the Energy Hub concept as defined by Geidl et al., (2007) [25]. In the Energy Hub concept there are 'three main entities: the energy supply, the energy demand and the energy conversion, storage and regulation', which can be described via different matrix formulations [20]. Fabrizio et al., (2009) [20] mentions that it is possible to determine the optimal configuration (in terms of costs or emissions minimisation) of such an energy system 'if the prices and characteristics of the energy conversion technologies and energy carriers are known'.

In order to then define the optimal design and operation of the MES, MILP formulations are used for solving the optimization problem. MILP formulations are used as they reduce the computation time, because of the use of both discrete values (integers) and linear models to describe processes. The necessary linear models for the MES optimization are mainly based on those defined by [23] [24] [22] [65] and implemented in the most recent version of the Energy Hub tool. New linear models or formulations (e.g. for the biomass gasification process) are developed and added to these already existing linear formulations.

The most recent version of the Energy Hub tool with aforementioned formulations is used in this research as it already contains an extensive set of energy conversion technologies and carriers. Also, the most recent version allows for the use of hourly input data (e.g. weather data), while still making sure that computation time is not considered too long by splitting up the operational variables into ones related and unrelated to binary variables [23]. Those related to binary variables include the on/off status and input/output power of energy technologies (e.g. electrolysers, gasifiers), while those unrelated to binary variables include the decision variables related to the amount of energy to be demanded, stored and imported/exported. By limiting the operational variables related to binary variables by using design days (instead of hours), the computation time is drastically reduced (ibid), making the use of this current version of the Energy Hub tool feasible and appropriate in this research. For this research, 30 design days are used to balance between computational time and model accuracy.

3.1.2 Optimization problem

The goal of the optimization of the design and operation of the MES is to minimize the total costs J, which is composed of the capital costs J_c, the operational costs J_o and the maintenance costs J_m, while making sure that constraints are met. Also, a multi-objective optimization is performed where emissions are taken into account by making use of the ϵ-constraint method [22], in which the trade-off between costs and emissions can be made with the creation of a Pareto front, which is elaborated on later in section 3.1.3.

The capital costs are defined as followed:

$$J_c = \sum_{i \in M} (\lambda_i \cdot S_i + \mu_i)\omega_i \tag{5}$$

In which the λ_i and the μ_i are respectively the variable and fixed cost coefficients, S_i the size of the technology (usually in kW) and ω_i the annuity factor. These costs are summed for each $i - th$ technology of the total technology set M.

The operational costs are calculated using the following formula:

$$J_o = \sum_{j \in N} \sum_{i \in M} \sum_{t=1}^{T} (u_{j,t} U_{j,i,t} - v_{j,t} V_{j,i,t}) \Delta t \tag{6}$$

in which u_i and v_i are respectively the import and export prices for power or energy and U_i and V_i are the amounts of imported and exported power or energy for the $j-th$ energy carrier in the total energy carrier set N for each time step t.

The maintenance costs are defined as:

$$J_m = \sum_{i \in M} \psi_i \cdot J_{c,i} \tag{7}$$

in which the maintenance costs are defined as a fraction ψ of the capital costs for each $i-th$ technology.

Next to this, the emissions (e) are determined according to the following equation:

$$e = \sum_{j \in N} \epsilon_j (\sum_{i \in M} \sum_{t=1}^{T} U_{j,i,t} \Delta t) \tag{8}$$

In which ϵ is the emission factor for each of the different energy carriers j.

Input and decision variables

To solve these equations, input variables are required. The *input variables* include 1) the prices and emission factors of the different energy carriers; 2) the prices for the different technology components (variable and fixed capital costs, maintenance costs); 3) the expected energy demand (i.e. the methanol demand) and finally the weather conditions for the different (renewable) energy technologies: solar irradiance profiles, wind speeds, temperatures and humidities (all on hourly basis).

The *decision variables* include 1) the selection of the different technologies; 2) the sizes of the technologies (in kW); 3) the schedules and on/off status of the different technologies and finally 4) the consumption and import of biomass, gas and electricity including the amount of energy stored (which can be in the form of hydrogen or electricity).

Constraints

In this optimization, boundaries, or so called constraints, for optimization exist. The most important constraints include the carrier constraint, which is related to the emissions and import of the energy carrier. Besides, there is the component constraint, which is related to the performance of the different energy conversion and storage technologies, described via the aforementioned linear formulations. Furthermore, there is the area constraint. The port and industrial cluster of Rotterdam has limited area for renewable energy sources. This needs to be taken into account in the analysis. Besides the industrial cluster of Rotterdam, there is also a different area constraint for offshore wind turbines. Finally, there is the energy balance, making sure that the produced and imported energy equals the exported and used energy at each given moment in time.

Solving this problem, using above mentioned information (equations, input variables & constraints), should provide insights in the most cost-effective design and operation of a multi-energy system used to produce low-carbon methanol in the port and industrial cluster of Rotterdam.

3.1.3 Multi-objective optimization

In the aforementioned cost optimization, emissions are not used for determining the optimal design. However, by making use of the aforementioned ϵ-constraint method, they can be included in the analysis. This makes sure that both a cost-effective, as well as a low-emission design for the production of methanol is realised. This is done by first optimizing solely for costs and determining the according emissions and costs. After that, an optimization is done solely for emissions, where also the according emissions and costs are determined. This results in a range in which the cost optimization gives the lowest costs with the corresponding maximum emissions, while the optimization for emissions gives the lowest emissions with the corresponding maximum costs. This range can then be used to define a certain number of emission constraints. Then the optimization for costs is performed again, resulting in a number of points on a so-called Pareto front in which emissions and costs are plotted against one another to see the impact of reducing emissions on the costs and vice versa for the optimal configuration of the MES for the production of low-carbon methanol in the port and industrial cluster of Rotterdam. This helps in deciding upon the trade-off between costs and emissions for the optimal design of a MES and can therewith be used to answer the main research question.

3.1.4 Branch & Bound for solving the optimization problem

This section elaborates on the actual solving of the optimization problem. A MILP problem, like the one described in sections 3.1.2 and 3.1.3, is usually solved via the branch & bound method [27]. In this method, the solving starts with the original MILP problem. As it is initially not clear how to solve this problem, the branch & bound method relaxes the integrality restrictions of the problem in a so-called *linear programming relaxation*. This means that decision variables are free to acquire other values than integer values. In that way, it becomes easier to solve the problem. The program then solves the problem, usually resulting in one or more of the decision variables not being an integer value. These variables are known as *branching variables* and are used for further analysis, where the branching variable is given an upper and lower constraint. For example, if one of the decision variables in the optimal solution has a value of 3.2, an upper and lower constraint of respectively 4 and 3 is set for further analysis, creating two new MILP sub-problems, which can be described as different nodes. Then these two problems, with known values for one or more of the decision variables are solved again, using the same procedure until there is a viable solution that yields the best objective value. If Gurobi considers one of the solutions as unfeasible (i.e. not meeting constraints other than the integrality constraint) it fathoms and discards them. When a solution to one of the sub-problems meets all the constraints and yields the best objective value up until that moment, that solution is regarded as the *incumbent* and is also fathomed in the solution tree, meaning that it does not need further branching. Every time the solver finds a solution that exceeds the outcome of the former incumbent, the incumbent is replaced. In the end, the Gurobi solver aims to converge to one solution by solving and discarding all the different MILP sub-problems until that point where the gap between the incumbent (also known as the upper bound) and second-best solution (lower bound) is approaching zero (MIP gap). At this point, optimality is demonstrated and a feasible and optimal solution is found [27]. This is summarized in Figure 4, to provide a clearer visualization of the processes.

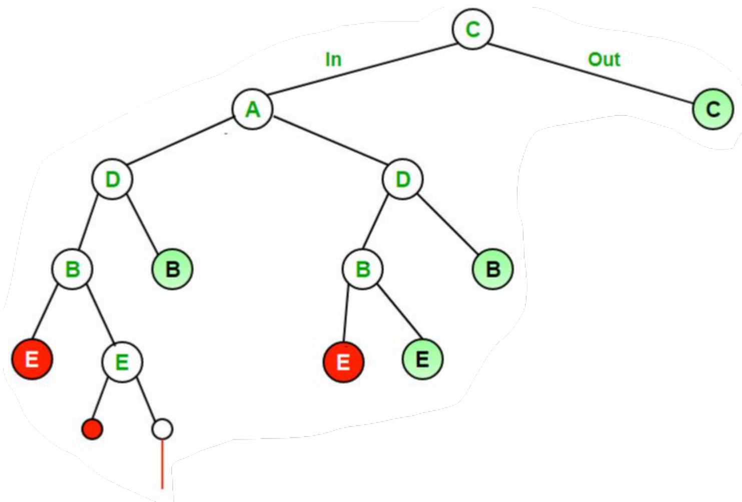

Figure 4: Branch and Bound tree with red nodes representing infeasible solutions and green nodes representing feasible, yet discarded solutions

3.2 Modelling of new components

To run the simulations and determine the optimal design for a MES concerning the production of low carbon methanol, two new components have to modelled and added to the Energy Hub tool (see section 3.1). The explanation on the modelling approach is explained in the sections below.

3.2.1 Parameter specification for the biomass gasification component

To determine the performance of the biomass gasification plant and the subsequent methanol synthesis, this research makes use of key performance indicators (KPI), used to describe the energetic requirements for the production of 1 kWh of methanol. The performance indicators for an integrated biomass gasification plant (including the methanol synthesis) include the indicators for the electricity, heat (in the form of steam), biomass and in one of the routes, hydrogen consumption per kWh of methanol.

To determine these performance indicators, this research makes use of parametric correlations, formulated by Sreejith et al., (2012) [54] and Sreejith et al., (2014) [55]. Sreejith et al., (2012) performed a regression analysis on the correlation between the independent variables of the steam biomass ratio (SBR) (in kg steam input per kg of biomass input) and biomass type (in %C, %O & %H of the particular type of biomass) on the dependent variables of synthesis gas output (in both dry gas volume per kg of biomass input (Nm^3/kg) and molar composition (mol%)). This regression analysis is based on the outcomes of a non-linear model, used to describe gasification processes [54] [55]. Sreejith et al., (2012) and Sreejith et al., (2014) finds that a high SBR typically results in a higher hydrogen content and lower biomass consumption, while at the same time resulting in a higher consumption of steam (i.e. heat). The opposite is true for a lower SBR. With regards to the biomass composition, the statement can be made that a high hydrogen content is preferred, as it results in high hydrogen and lower CO_2 yields. Therefore, in this research, the impact of changing the SBR and biomass type on both the performance indicators of the biomass gasification process (e.g. kg biomass/kWh methanol), as well as the optimal design of the MES, is assessed. Therewith, it tries to give an answer to the first sub-question, formulated in the introduction.

The optimal SBR for methanol production from biomass gasification using fluidized beds differs significantly between researchers. Al Nous et al., (2019) and Puig-Gamero et al., (2018) [47] [1] mention optimal ratios of 0.9, while another researcher puts the optimal value between 0.4 and 0.5 [68]. Molino et al. 2018, [41] mentions an optimal value somewhere between 0.3 and 1. Therefore, as all the other values found also differ between 0.3 and 1, the SBR in this research is varied between 0.3 and 1. For the biomass types, three different types with different carbon, oxygen and hydrogen contents are assessed and further elaborated on in section 3.3. The gasification temperature is set at 825 ℃, as the earlier references mention temperatures between 750 and 900 ℃[1] [47] [68]. This temperature is fixed during the research. For the carbon conversion efficiency (CC) (amount of carbon converted from solid biomass into gaseous form in the synthesis gas), the assumption is made that it is fixed at 90 %, as this is a typical value for the associated gasifier temperature and gasification agent (i.e. steam) [1] [47].

The parametric correlations for the molar composition of the synthesis gas are represented as follows:

$$CO_{2_{mol\%}} = 40.14 + 0.22C - 5.13H + 0.54O - 0.02T + 3.02SBR - 0.04CC \tag{9}$$

$$CO_{mol\%} = -21.19 - 0.13C + 4.17H - 0.30O + 0.03T - 4.47SBR + 0.16CC \tag{10}$$

$$H_{2_{mol\%}} = 27.28 + 0.08C + 2.50H - 0.44O + 0.01T + 2.03SBR + 0.24CC \tag{11}$$

in which C, H and O are given in mass percentages of the dry biomass, T is given in Kelvin and SBR is given as the ratio between steam and biomass (kg/kg) [54] [55]. These linear approximations are based on the aforementioned regression analysis of thirty different types of biomass and could therefore, to a minor extent, differ in correlation between the different types of biomass.

An example in which the linear approximation (based on the equations above) and the non-linear outcomes of the model of Sreejith et al., (2012) and Sreejith et al., (2014) are set out to one another is shown in the figure below.

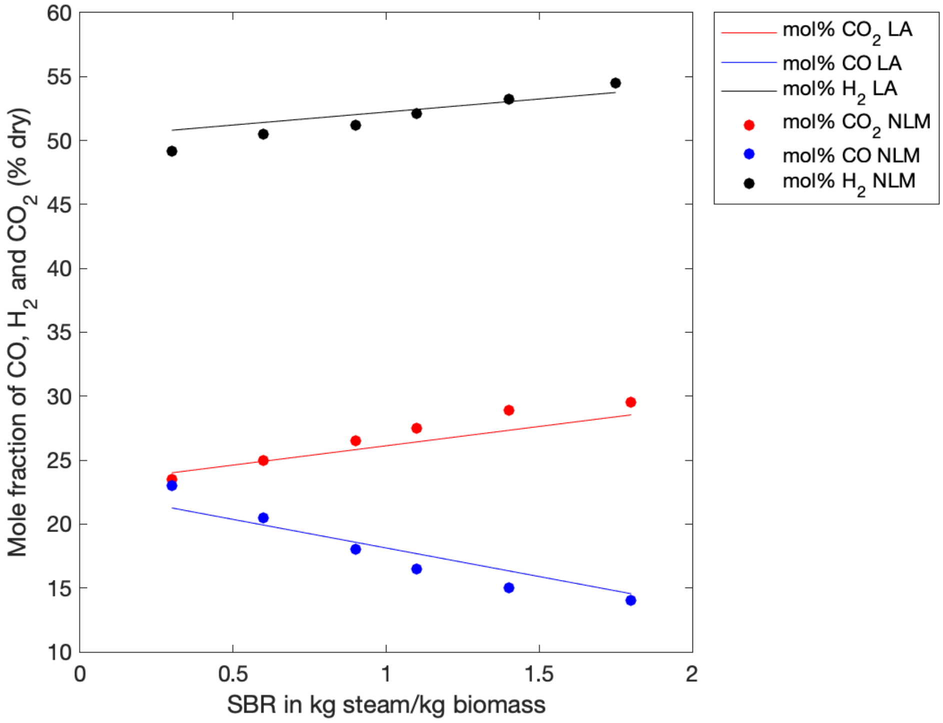

Figure 5: Example of the linear approximation (LA) set out against the outcomes of the non-linear model (NLM) for one biomass type

To determine the molar output (MO) (in moles/kg biomass) in terms of dry synthesis gas, this research assumes the volumetric outputs (in Nm^3/kg biomass) presented in Sreejith et al., (2012). This number is then multiplied with the molar volume (MV) to obtain the molar output in terms of dry synthesis gas [54]. Calculations are performed according to the following equations.

$$MO(SBR, MV) = \begin{cases} 1.35 \cdot MV & \text{if SBR} = 0.3 \\ 1.41 \cdot MV & \text{if SBR} = 0.53 \\ 1.46 \cdot MV & \text{if SBR} = 0.76 \\ 1.50 \cdot MV & \text{if SBR} = 1 \end{cases} \tag{12}$$

In this research, a fixed molar volume of 0.023645 Nm^3/mol is used, as the volumetric outputs in Sjeerith et al., (2012) are given in Nm^3. Together with the outputs of equations [9-11], it is also possible to calculate the amount of moles of each individual molecule (i.e. CO, CO_2 & H_2) per kg of biomass input.

To then calculate the KPIs for the production of 1 kWh of methanol, it is key to know the synthesis gas composition that is used as an input in the methanol synthesis reactor. Machado et al., (2014) [38] & Zhang et al., (2020) [66] mention different synthesis gas compositions. The former presents a synthesis gas composition for the hydrogenation of both CO & CO_2 and therefore has a slightly lower performance (due to the reduced performance of the catalyst). This composition is used for the hydrogen addition route. The latter presents a synthesis gas composition mainly for the hydrogenation of CO, leading to higher performances. This composition is used for the CO_2 scrubbing (and compression) route. The synthesis gas composition as well as the synthesis gas requirement (mol synthesis gas/kWh methanol) is presented in the table below.

Table 1: Synthesis gas composition for the two different gasification routes

Component	mol% CO_2 scrubbing (& compression)	mol% H_2 addition
H_2	67	70
CO	30	17
CO_2	3	13
Molar mass	10.80 g/mol	11.89 g/mol
Route	mol syngas/kWh methanol	
CO_2 route	17.78	
H_2 route	18.00	

This can then be used to determine the key performance indicators (KPIs) for the production of 1 kWh of methanol. It is assumed that In the CO_2 scrubbing and capture route, the hydrogen demand (11.92 moles H_2/kWh MeOH, as per the table above) should at least be covered by the biomass input (B_i), as no extra hydrogen is added. The excess CO production in this case is considered to be small enough to get discarded, but in reality, it does slightly impact the gasification process, typically leading to lower yields. The excess CO_2 is scrubbed and potentially compressed. In the hydrogen addition route, the amount of **biomass** (in kg) to produce 1 kWh of methanol should be able to cover the demand for CO (3.06 moles CO/kWh MeOH, as presented in the table above) and is calculated accordingly. The extra required hydrogen is added to the mixture and the excess CO_2, which is typically really minor, is discarded. Based on this, it is possible to calculate the amount of **steam** and consequent heat consumption (Q). Based on Sreejith et al., (2012) [54], in all cases steam is supplied at a pressure of 1 bar and a temperature of 350 °C. Based on the superheated steam table, this results in a energy content of 0.8805 kWh/kg steam. The steam consumption is then:

$$Q = (SBR \cdot B_i) \cdot 0.8805 \tag{13}$$

Regarding **electricity** consumption, Hannula et al., 2013) [28] presents the following processes that consume electricity (see Table below).

Table 2: Electricity consumption in integrated BtM plant

Process	Consumption (kWh/kWh methanol)
Biomass drying	0.012
Synthesis gas compression	0.081
Acid gas removal	0.004
Methanol synthesis	0.003
Miscellaneous	0.012

To compress the CO_2 for later use (applicable for the CO_2 scrubbing route compressing and utilising the CO_2, 0.1 kWh/kg CO_2 is required [28].

To cover the **hydrogen** demand in the hydrogen addition route, the difference between the demand for hydrogen and the already produced hydrogen in the gasification process (in moles) is calculated and added to the mixture to get to the right amount of hydrogen. To determine the energy requirement in the form of hydrogen, the LHV of 120 MJ/kg is assumed [2].

Finally, **CO_2 production** is defined based on the excess CO_2 in the mixtures after gasifying the required amount of biomass. This excess CO_2 can either be scrubbed and discarded. In another route, the CO_2 is compressed and can be used either somewhere else within the system boundaries or stored underground. If a remainder then still exists, it is discarded according to the following equation:

$$CO_{2_p} = CO_{2_d} + CO_{2_l} \tag{14}$$

In which the subscripts p, d and l respectively indicate the produced CO_2, the discarded CO_2 and the CO_2 going to the load (within the system boundaries). CO_2 that is going to the load and is being captured and stored underground is seen as a form of negative emissions, as the emissions associated with biomass (gasification process) are seen as carbon neutral and can therefore be negative if stored underground.

The KPI of each *i-th* energy carrier for the production of 1 kWh methanol can therefore be described as a function of the SBR (S), type of biomass (B) and gasification mode (GM) (e.g. adding hydrogen or scrubbing/compressing CO_2):

$$KPI_i = f(S, B, GM) \tag{15}$$

The key performance indicators (e.g. kg biomass/kWh of methanol) for each of the types of biomass, SBR and gasification mode are based on the information, presented above and are shown in Appendix A1.

3.2.2 Integration of biomass gasification component in EHub

To integrate the different gasification modes, including its KPIs, in the EHub, three different components are constructed. These three different components are 1) the biomass gasification component in which the produced CO_2 is scrubbed; 2) the biomass gasification component in which the produced CO_2 is scrubbed and captured and 3) the biomass gasification component in which hydrogen is added. The KPIs for each component, each type of biomass and corresponding SBR are precalculated based on the information and equations provided in the section before. All components have the possibility to run on one of three types of biomass and one of four different SBRs (0.3, 0.53, 0.76 and 1), which means that twelve different sets of KPIs per component are available (as is shown in Appendix A1). The type of biomass is always fixed for the simulations, but the SBR can either be fixed, or used as a decision variable as to decide which SBR is the preferred one in the optimization of the MES. It is assumed that the operating SBR cannot change during the time of operation; ergo, it is fixed for the full time frame of the simulation. Finally, the different gasification components are constrained by start-up, shut-down and ramping times, as mentioned in section 2.2.

The integration of the different components, including its constraints, in the EHub is explained below via the use of several equations. These equations hold for all three components inside the EHub; the only difference resides in the associated KPIs that are being used to calculate the costs, energy consumption and emissions.

The hourly methanol output $P_{MeOH,t}$ (in kWh MeOH) is described by the following equation:

$$P_{MeOH,t} = \sum_{m=1}^{M} x_m L_t \tag{16}$$

$$x_m \in \{0; 1\} \tag{17}$$

In which the x_m is a binary variable, of which subscript m denotes the operating mode (i.e. the used SBR and its corresponding KPIs) and L_t the hourly load. M denotes the total amount of operating modes, which, in this case, is equal to 4. As mentioned, it is not possible to switch the operating modes during the simulated time frame. Therefore, the sum of all x_m should be equal to 1

$$\sum_{m=1}^{M} x_m = 1 \tag{18}$$

Another constraint is related to the hourly load. This hourly load cannot exceed the installed capacity (C_i) of the MeOH plant and must be a positive value (higher than 0).

$$0 \leq L_t \leq C_i \tag{19}$$

Since there are multiple operating modes x (4 modes), an alteration of equation 16 is needed. This is because equation 16 now contains bilinearity of two decision variables (hourly load and operating mode). This must be altered in order to be modelled in a linear program, feasible for the EHub tool. Glover et al., (1975) [26] has formulated a way to do so by reformulating the product of the two decision variables of equation 16 (i.e. the operating mode and hourly load) into an new, merged variable named $\widetilde{L_{\mathrm{t,m}}}$. This reformulates equation 16 as follows:

$$P_{MeOH,t} = \sum_{m=1}^{M} \widetilde{L_{t,m}} \tag{20}$$

In order to meet the constraint formulated in equation 19, the installed capacity must also be multiplied with the operating mode x_m, leading to a new constraint:

$$0 \leq \widetilde{L_{t,m}} \leq x_m C_i \qquad \forall m, t \tag{21}$$

This brings another bilinearity, as the installed capacity and operating mode are now multiplied with one another. This can be solved with the same procedure as before in which the product of the two decision variables is replaced by a new, merged variable named $\widetilde{C_{\mathrm{i,m}}}$, which reformulates equation 21 as follows:

$$0 \leq \widetilde{L_{t,m}} \leq \widetilde{C_{i,m}} \qquad \forall m, t \tag{22}$$

Now, it is key that both the load and installed capacity are bound to an upper and lower limit. The load is already bound by an upper and lower limit as displayed in equation 22. To bound the installed capacity $\widetilde{C_{\mathrm{i,m}}}$, two extra constraints are formulated:

$$C_i^{min} x_m \leq \widetilde{C_{i,m}} \leq C_i^{max} x_m \qquad \forall m \tag{23}$$

$$C_i - C_i^{max}(1 - x_m) \leq \widetilde{C_{i,m}} \leq C_i \qquad \forall m \tag{24}$$

Now that the hourly methanol output, load and capacity are properly described, it is possible to describe the electrical, thermal, (hydrogen) and biomass inputs to the gasification system, as well as the CO_2 output. These are described, respectively by the following equations:

$$E_{el,t} = \sum_{m=1}^{M} \epsilon_{m,el} \widetilde{L_{t,m}} \tag{25}$$

$$E_{th,t} = \sum_{m=1}^{M} \epsilon_{m,th} \widetilde{L_{t,m}} \tag{26}$$

$$E_{H2,t} = \sum_{m=1}^{M} \epsilon_{m,H2} \widetilde{L_{t,m}} \tag{27}$$

$$E_{b,t} = \sum_{m=1}^{M} \epsilon_{m,b} \widetilde{L_{t,m}} \tag{28}$$

$$E_{CO2,t} = \sum_{m=1}^{M} p_{m,co2} \widetilde{L_{t,m}} \tag{29}$$

In which the ϵ and p denote the preprocessed KPIs, defined for each type of biomass, gasification component and operational mode m (SBR).

To finish the model, technological dynamics are added to the model to make sure that the operation of the gasifier at part load or during shut down and start up is modelled in a realistic fashion. The dynamic behaviour is described in terms of (1) the operating ramp constraints (ramp-up and ramp-down constraints, (2) the start-up ramp constraint (increasing power) and (3) the shut-down ramp constraint (decreasing power), as introduced in section 2.2. All equations for describing the technological behaviour are based on the equations provided by Arroyo et al., (2004) [4] (equations 1-12 in that paper) and implemented in the EHub by Gabrielli et al., (2018) [24].

To conclude the modelling of the biomass gasification component, a flow diagram of the presentation of the component is given below.

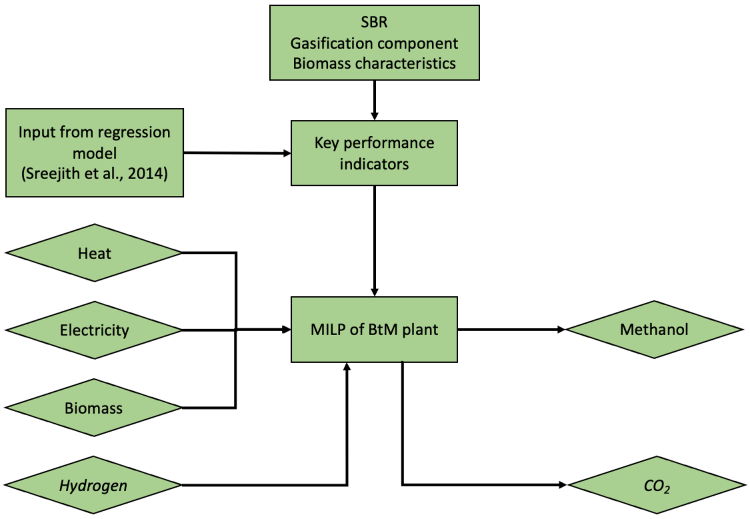

Figure 6: Flow diagram showing the MILP of the BtM plant to be assessed in this analysis

3.2.3 Parameter specification of the CO_2 hydrogenation component

Besides the gasification component, a CO_2 hydrogenation component is also added to see if and to what extent synergies between the two methanol production technologies exist.

The CO_2 hydrogenation component is modelled via a black box approach, where CO_2 and H_2, together with electricity, are consumed to generate methanol. Besides CO_2 and H_2, there is a production of heat. This heat production, however, is internally used for the distillation of the methanol later on in the process. This means that the heat remains in the black box and is not considered an in- or output [15]. Key performance indicators for the CO_2 hydrogenation component are retrieved from a technology factsheet from the TNO and are presented below [15].

Table 3: Key performance indicators for the CO_2 hydrogenation component

Carrier	Value	Unit
CO_2	0.256	kg CO_2/kWh MeOH
H_2	1.239	kWh/kWh MeOH
Electricity	0.051	kWh/kWh MeOH

3.2.4 Integration of the CO_2 hydrogenation component in the EHub

The implementation of these KPIs in the EHub tool takes a similar, yet simpler, approach as the approach used to implement the biomass gasification component. This is because there are no different operating modes associated with the CO_2 hydrogenation component. The hourly methanol output can therefore simply be described as:

$$P_{MeOH,t} = L_t \tag{30}$$

In which L denotes the hourly load of the methanol plant. The load should conform to the following bounds:

$$0 \leq L_t \leq C_i \tag{31}$$

In which C_i is equal to the installed capacity of the methanol synthesis plant.
The hourly inputs regarding H_2, CO_2 and electricity are denoted as follows:

$$E_{H2,t} = \epsilon_{H2} L_t \tag{32}$$

$$E_{CO2,t} = \epsilon_{CO2} L_t \tag{33}$$

$$E_{el,t} = \epsilon_{el} L_t \tag{34}$$

In which the ϵ are the KPIs as presented in table 3. The simplified flow diagram for the synthesis plant is visualized in the figure below.

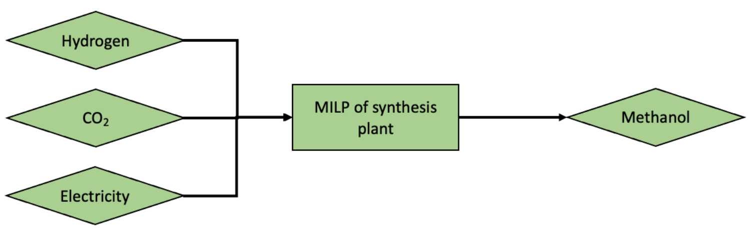

Figure 7: Flow diagram showing the MILP of the methanol synthesis plant running on CO_2 and H_2

3.3 Data Collection & Case Studies

This section elaborates on the data collection & case studies for the MES optimization. The first subsection explains the data collection for the energy carriers, while the second subsection focuses on the data collection for the energy technologies. The final subsection elaborates on the case studies, including the system boundaries related to the methanol demand & area constraints (i.e. for the installation of renewable energy technologies) in the industrial cluster of Rotterdam.

3.3.1 Energy Carriers

Data collection takes place on a quantitative basis, as that forms the input in the optimization problem (see input variables in section 3.1). Price and emission data for the energy carriers is collected for the year 2019. Although future prices and emission factors for energy carriers might change the optimal design, the large uncertainties associated with it would drastically decrease the reliability of the outcomes of this research. Biomass prices, however, are altered in a sensivity analysis to see how and to what extent it changes the optimal design of the MES.

Data regarding **electricity** & **gas** prices is collected, respectively via the European Network of Transmission System Operators for Electricity (ENTSO-E), where hourly electricity prices and day-ahead markets prices are available in large databases and Statista, where the average Dutch gas price (2019) is considered for the analysis [56][19]. When looking at the emissions from the generation of electricity, this research takes an average yearly value of 0.43 kg CO_2/kWh_e, as is determined by the CBS for the year 2019 [11]. The gas emissions are set at 0.20 kg CO_2/kWh [52]. Finally, it is assumed that there is no constraint on the import of electricity or gas from the grid.

Regarding **biomass** as an energy carrier, the assumption is made that biomass emissions are purely based on the emissions occurring during the transport over water (from port to port). The reason for this is that biomass emissions, occurring during the harvesting, pre-processing and land transport, are hard to generalize for the different types of biomass, as there are a lot of uncertainties related with it. Emissions for international transport on the other hand are easier to generalize, due to fact that all types of biomass are typically transported by ships, that have a standard emission factor per tonne km. Biomass costs are based on the costs for the feedstock, the handling of the feedstock and the transport of the feedstock. In reality, the supply chain of biomass is a much more complex system, typically resulting in higher cost & emission estimations, but due to the scope of this research (which is more focused on the optimization of the design of an energy system as opposed to the optimization of the supply chain), simplifications are made. In the analysis, three types of biomass are assessed and used in the optimization problem. The types of biomass come from multiple regions in the world and have different prices, transport emission factors and compositions. This is to see whether different types of biomass impact the optimal design of the MES. The main requirements in picking the types of biomass are based on the availability of the biomass type; it should be able to meet large quantities of methanol demand. Also, it should be considered a waste product from either agriculture or forestry.

The first type of biomass in this research is sugarcane bagasse from Colombia. Sugarcane bagasse is a waste product from the production of sugarcane, the second most produced commodity crop in the world with an annual worldwide production of 1.89 billion tonnes of sugarcane in 2016 [42]. Around 23 million tonnes of the total sugarcane production is produced in Colombia [57]. 27% of that mass is eventually converted into sugarcane bagasse, meaning that there is a vast availability of the resource, which makes it an interesting feedstock for the production of methanol [42].

For the bagasse prices, data from a study by the Wageningen University (WUR) is used [18]. This study researched the export potential and costs for biomass (i.e. sugar cane bagasse and oil palm residues) from Colombia to the Netherlands. They find that the costs for processing and transporting sugar cane bagasse from Colombia to Rotterdam are valued at €133.76/tonne bagasse pellet delivered to Rotterdam. This same research assumes the lower heating value (LHV) of non-processed bagasse (50% moisture content) at 8 MJ/bagasse (or 17.5 MJ/kg of processed pellets), leading to a price of €7.64/GJ or €0.1338/kg for the sugar cane bagasse. Assuming an emission factor of 0.015 kg CO_2/tonne km pellets and a nautical distance of 11,380 km (Puerto Bolivar - Rotterdam), the emissions for bagasse transport result in 0.1707 kg CO_2/kg bagasse [18].

Another type of biomass is wood residue from Finland [28]. According to Hannula & Kurkula (2013), Finland produces on average 30 to 50 m^3/km^2 of sustainably produced logging and wood residues on an annual basis. This translates to an average of 67.5 MWh/km^2 of biomass harvesting potential (LHV 16.33 MJ/kg), making it an interesting biomass source for the production of liquid fuels, such as DME, FT-fuels & methanol [28]. According to the same source, the costs for the biomass fuel, including the processing, handling and land transport of the wood residues, is equal to €0.0767/kg. Assuming a bulk transport shipping cost of 0.0032 EUR/tonne km [40] and a nautical distance of 2600 km (Helsinki - Rotterdam), the total costs are estimated at €0.0848/kg wood residues. Assuming the same emission factor of 0.015 kg CO_2/tonne km, the transport emissions are set at 0.0408 kg CO_2/kg wood residue.

The final type of biomass is rice straw from Indonesia. Rice straw from Indonesia can be seen as an abundant source of potential biomass energy. This is because, on an annual basis, Indonesia produces roughly 100 Mtonnes of rice straw [3]. According to a report by the Ministry of Economic Affairs in the Netherlands on the potential of rice straw as a feedstock in the biobased economy, the total costs (excluding shipping costs) are estimated at €0.0533/kg (LHV of 14 MJ/kg), making it also quite a cheap source of biomass energy [7]. The main downsides of rice straw include the relatively low energy content (LHV 14 MJ/kg) as compared to the other types of biomass and the relatively high shipping costs, as most of the rice (straw) is produced in South-(East) Asia. Assuming a nautical distance of 16,450 km (Jakarta - Rotterdam), and the same shipping costs of 0.0032 EUR/tonne km, the total costs for Indonesian rice straw are set at €0.1058/kg. Assuming the same emission factor of 0.015 kg CO_2/tonne km, the transport emissions are set at 0.2489 kg CO_2/kg rice straw.

Biomass shipping & storage capacity port of Rotterdam

Biomass availability alone is not enough to be feasible for the production of large amounts of methanol. This is because the biomass also needs to be transported and stored for later use. According to sources from the Port of Rotterdam [45], the port has the ambition to handle 8 to 10 million tonnes of biomass in 2020, as the port aims to be not only a user, but also distributor of biomass for the rest of North-West Europe. With ships, used for the transport of pelletized biomass or bales (e.g. bagasse pellets), being able to transport 80.000 tonnes per shipment [45], it is assumed that there is both enough shipping and storage capacity to handle the biomass flows used for methanol production.

The costs & emission factors (transport emission factors if it concerns biomass carriers) for the energy carriers, as well as the composition of the assessed biomass types, is displayed in the tables below.

Table 4: Costs & emission factors of the different energy carriers

Carrier	Price (€ /kWh)	Emission factor (kg CO_2/kWh)	Reference
Electricity	0.06 (avg.)	0.43	[19] [11]
Natural gas	0.0416	0.20	[12] [52]
Carrier	Price (€ /kg)	Emission factor (kg CO_2/kg)	Reference
Sugar cane bagasse	0.1338	0.1707	[18]
Nordic wood residue	0.0848	0.0408	[28] [40]
Rice straw	0.1058	0.2489	[7] [3]

Table 5: Composition of the different types of biomass based on ultimate analysis (mass percentage)

Biomass type	%C	%H	%O	Reference
Sugar cane bagasse	46.96	5.72	44.05	[42]
Nordic wood residue	51.30	6.10	40.85	[28]
Rice straw	42.63	5.61	39.40	[54]

3.3.2 Energy Technologies

This section elaborates on the data collection related to the energy technologies. First of all, to determine the performance of the different *renewable* energy & conversion technologies, weather data is required. For calculating the output of solar PV panels for example, temperature and solar irradiance profiles are required. For the wind turbines, wind speed profiles are needed. Finally, for the performance of the DAC, the relative humidity of the ambient air is required. The required weather data is collected from the KNMI data bases for the year 2019 [36]. The required input data for the Rotterdam region (weather station 344) is summarized in the figure below. For the offshore wind profiles, data from the Hoorn-Alfa weather station is used. The offshore wind turbines are modelled as the only other, separate node providing electricity to the main node (e.g. industrial cluster).

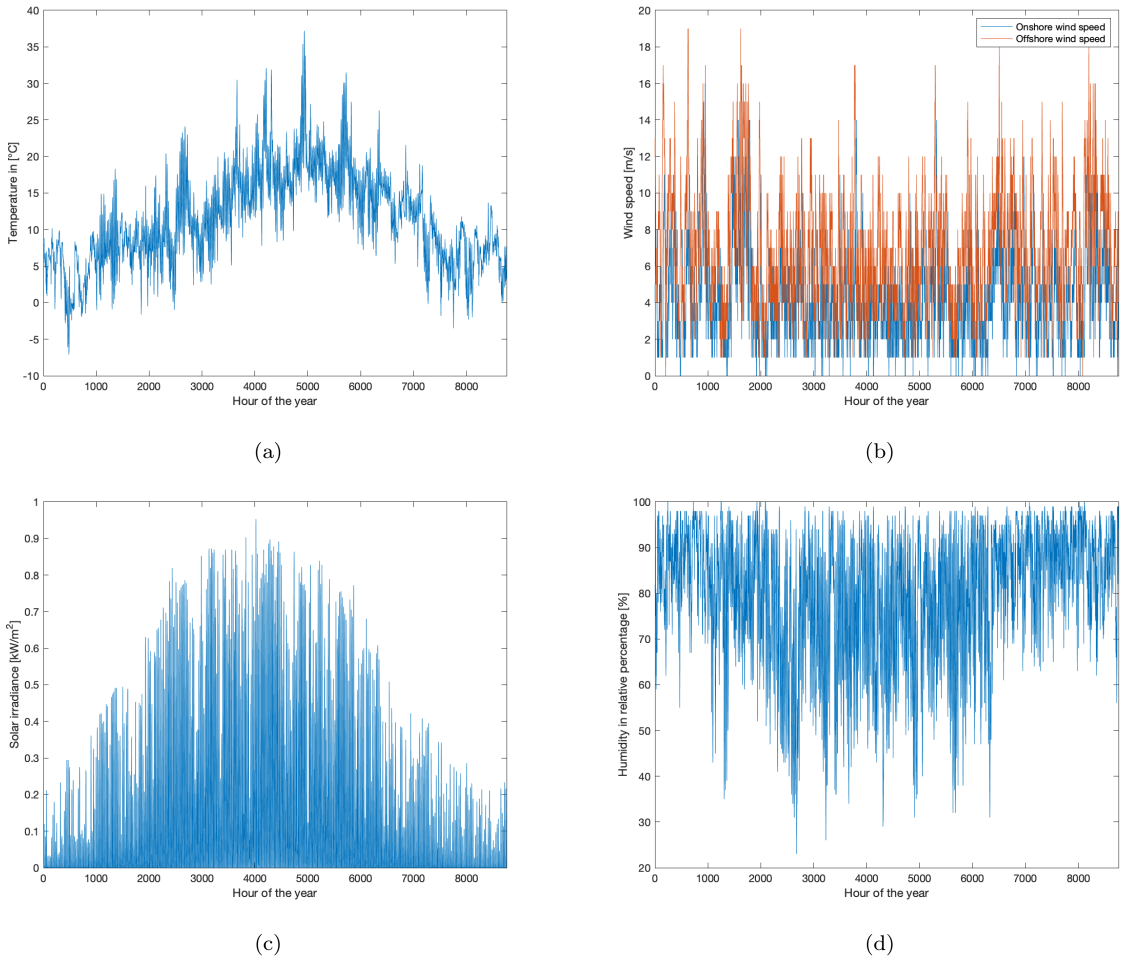

Figure 8: Weather input data for the year 2019 in the Rotterdam region with figure (a) displaying the annual temperature profile, figure (b) displaying the annual wind profile for both offshore (orange) and onshore (blue) weather stations, figure (c) displaying the solar irradiance profile and figure (d) displaying the relative humidity

To continue, the data regarding the technology components is collected either via already existing data in the Energy Hub tool or via literature analysis into demonstration and commercial scale projects. The costs and performance indicators for the already existing technologies in the Energy Hub tool are based on existing data and are summarized in Appendix A2.

For the estimation of the investment costs for the new biomass gasification component, data from multiple reports regarding the cost estimates for biofuel production systems are used [30] [28]. Holmgren et al., (2015) [30] mentions figures between €2000-2300/kW output [30] for integrated biomass to methanol (BtM) production systems using CFB reactors as gasifiers. Costs differ due to the difference in deciding to scrub or not scrub and compress or not compress the CO_2 during the process of acid gas removal. Another report by Hannula et al., (2013) [28] finds an average value of €2000/kW for the integrated process of converting biomass to methanol. The analysis of these processes in both the cost estimates of Holmgren et al., (2015) and Hannula et al., (2013), however, do concern the inclusion of oxygen production, which is not the case in this research. Hannula et al., (2013) [28] mentions that the costs for that particular part of the process are estimated at €256/kW. This paper also mentions that the compression of CO_2 on the other hand results in an increase in capital costs equal to €36/kW. Based on this, it is assumed that the base costs for a biomass to methanol plant is estimated at €1744/kW (€2000/kW minus the €256/kW for oxygen production). Costs increase with €300/kW if CO_2 scrubbing is applied and increase even further (with €36/kW) if CO_2 is also compressed for utilisation somewhere else. Maintenance costs are estimated at 3.5% of the total investment costs [31].

For the methanol synthesis reactor (i.e. the CO_2 hydrogenation component), cost estimates are based on the TNO technology factsheet and the report by Zhang et al., (2019) [67] [15]. The TNO technology factsheet [15] assumes a price of €342/kW (including fixed operational costs, such as employees and water treatment), while Zhang et al., (2019) [67] mentions a price of €330/kW. This research assumes the more conservative and complete figure by the TNO: €342/kW. Maintenance costs are estimated at 2% of the total capital investment costs [37].

One key note with these investment costs is the fact that these investment costs are all scaled to a specific size. In the case of Hannula et al., (2013) [28], the costs are scaled to a BtM plant with an output equal to 172 MW_{MeOH}, while the methanol synthesis reactor for the CO_2 hydrogenation is scaled to 333 MW_{MeOH} [67]. This report, as well as the report by Holmgren et al., (2015) [30] uses an average scaling factor (k) of 0.67 for the integrated Biomass-to-MeOH plant. To calculate the costs for smaller or larger size plants, the following equation is used:

$$C = C_0 * \left(\frac{S}{S_0}\right)^k \tag{35}$$

With C_0 being the total investment costs for a plant with size S_0 (172 MW_{MeOH} for the BtM plants and 333 MW_{MeOH} for the $CO_2 + H_2$ component) and scaling factor k.

To then calculate the investment costs for a certain methanol plant, a piecewise affine (PWA) approximation is implemented in the EHub to account for the size dependency of the capital cost [23]. This PWA is a linear formulation that accounts for the concavity of the investment cost function (equation 35) and is used to decide the fixed (independent of the size) and the variable (dependent on the size) investment costs for a plant with a certain size. For this research, four different PWA approximations are implemented for four different size ranges (S_{min} to S_{max}). The fixed and variable investment costs for each of the four PWA approximations, together with the corresponding size ranges are visualized and summarized, respectively in the graph and Table below.

Table 6: Fixed and variable investment costs for new components

Component	Fixed CAPEX (in M€)	Variable CAPEX (in € /kW)
BtM + H_2 addition	0; 53.2; 102.4; 157.3	2527; 1817; 1476; 1266
BtM + CO_2 scrubbing	0; 62.4; 120; 184.3	2961; 2130; 1730; 1484
BtM + CO_2 utilisation	0; 63.5; 122.1; 187.6	3014; 2167; 1760; 1510
$CO_2 + H_2$ component	0; 14.6; 27.3; 41.2	639; 445; 354; 299
Component	S_{min} (MW)	S_{max} (MW)
BtM + H_2 addition	0; 50; 150; 300	50; 150; 300; 500
BtM + CO_2 scrubbing	0; 50; 150; 300	50; 150; 300; 500
BtM + CO_2 utilisation	0; 50; 150; 300	50; 150; 300; 500
$CO_2 + H_2$ component	0; 50; 150; 300	50; 150; 300; 500

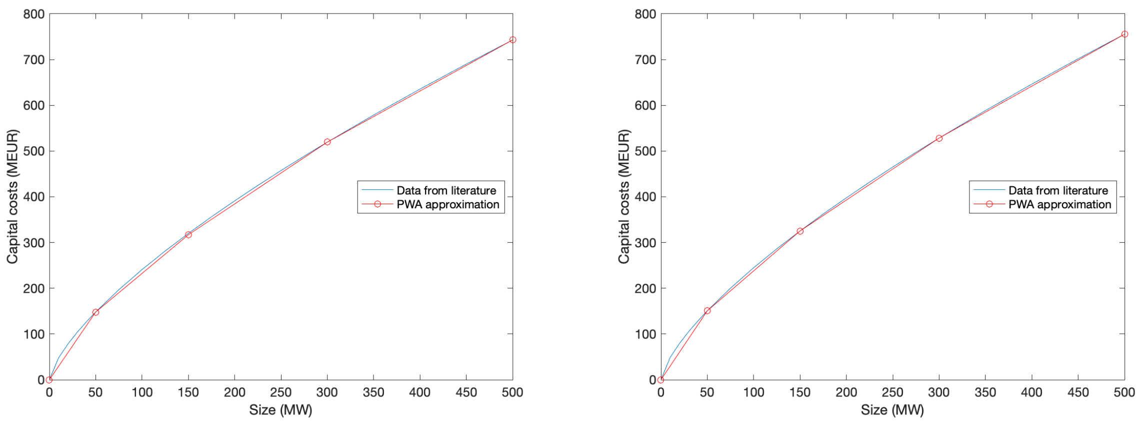

(a) (b)

Figure 9: PWA formulations for two exemplary energy technologies: (a) BtM + CO_2 scrubbing & (b) BtM + CO_2 utilisation and/or storage

3.3.3 Case studies

This section elaborates on the case studies to be assessed and the (geographical) characteristics of the industrial cluster of Rotterdam.

Geographical considerations: all the simulations in this research are done for the industrial cluster of Rotterdam. This industrial area has constraints in the deployment of on- and offshore wind turbines, as well as solar PV. According to the Port of Rotterdam, 400 hectares (or 4.000.000 m^2) of roofs and temporary fields are available for the production of solar energy [46]. Regarding space for wind turbines, it is assumed that there is space for 100 turbines with a power output of 3 MW [43]. Assuming an average of 8 MW/km^2 [17], 37.5 km^2 of space is available for the construction of new turbines. Regarding offshore turbines deployment, this research looks at the space reserved on the North Sea. According to a paper by the Ministry of Infrastructure and Environment, this is equal to 2900 km^2 [59].

When looking at the methanol output, this research takes the size of an average sized methanol plant. Although most methanol plants are currently operated using natural gas as an input, this research assumes that it it possible to obtain the same output figures for biomass gasification plants. According to Burridge et al., (2009), sizes for methanol plants differ between multiple ktonnes to more than 1 Mtonne per year [9]. This research assumes a yearly output of 400 ktonnes of methanol, in which it has to meet a constant hourly demand.

For this research, multiple simulations are performed to see how the system behaves in a changing environment. The simulations are performed with 30 design days (see section 3.1.1) and a MIP gap of 0.005 (section 3.1.4). All simulations are performed for **two** main cases, as already briefly explained in the introduction: a case with and a case without a carbon storage facility (from now on: carbon sink). As Rotterdam is planning on developing an offshore carbon sink (Porthos Project) in the North Sea, it is interesting to see how the in- or exclusion of that sink impacts the optimal design and operation of the MES. This helps in answering the sub-question related to the impact of a carbon sink on the optimal design and operation of a MES for low-carbon production.

Besides this distinction, the analyses (for both the in- and exclusion of a carbon sink) to be performed are as follows: first, for every type of biomass, the four different values for SBR (0.3, 0.53, 0.76 and 1) are used as a decision variable to see which is preferred when optimized for costs or emissions. For these analyses, a cost optimization, an emission optimization and a Pareto front are generated. Then, for each type of biomass, the used technologies, sizes and operation schedules are assessed and explained. This helps in answering the question on how the different types of biomass affect the optimal design and operation of the MES. After that, the system is assessed based on multiple fixed SBR values (as defined earlier) to see how the different SBRs impact the optimal design and operation of the MES, which helps in answering the sub-question related to the impact of the SBR on the optimal MES.

The analysis ends with a sensitivity analysis on different future scenarios. As current biomass prices are highly dependent on availability, harvesting and transport costs, the actual biomass prices might be different than those shown in this research. This could potentially lead to different outcomes concerning the optimal design and operation of the MES. Especially when looking into the future, biomass prices could rapidly change, due to increases or decreases in demand and availability. Duic et al., (2017), for example, mentions that it is expected that prices for sustainable biomass resources will increase if scarcity and demand for biomass resources continues to increase [16]. According to that research, prices for the Netherlands are expected to change between 20 and 30% in 2030, as compared to current prices.

Another uncertainty is related to the methanol output. As mentioned before, it is still uncertain to what extent it is possible to produce certain quantities of methanol, using biomass gasification plants. Also, it is uncertain to what extent the industrial cluster is planning on following the decarbonization scenario of becoming a major hub for the production of synthetic fuels. For that reason, the sensitivity analysis takes into account lower and higher methanol demands to see how and if it impacts the optimal design of the MES.

For both the case including and excluding a carbon sink, these alterations are implemented and assessed in a sensitivity analysis. This analysis is performed for the best type of biomass (in terms of costs and emissions) with the SBR being a decision variable, to see if and how the optimal SBR and design of the MES also changes.

4 Results

4.1 Impact of different types of biomass on optimal design of MES

This first section focuses on the impact of the different types of biomass on the optimal design of the MES for the production of low-carbon methanol. The system for which the results are generated resembles the one shown in Figure 3, section 2.4.

4.1.1 Optimal design of MES with inclusion of carbon sink

To start off, the optimization of the MES is performed with the inclusion of a carbon sink. Within this optimization, a multi-objective optimization is performed in which the costs are minimised for different emission constraints. These emission constraints differ per type of biomass, due to different emission factors for the import/transport of biomass. Figure 10 shows the so-called Pareto front for the three different types of biomass.

Based on this figure, it can be seen that the Nordic wood residue is the preferred type of biomass, both in terms of emissions and costs. This can mainly be explained by the fact that the Nordic wood residue is both the cheapest source of biomass (in €/kg import) and the type of biomass with the lowest transport emissions. This goes to show that the import of biomass from countries or places close by is preferred, as that results in the lowest costs and emissions. When comparing the Indonesian rice straw with the Colombian bagasse, it can be seen that rice straw is preferred, when emissions form no constraint, while the bagasse is preferred when emissions do form a stricter constraint. This can be explained by the fact that bagasse is considered a more expensive type of biomass, resulting in relatively high costs in situations with no emission constraints. On the other hand, rice straw has higher transport emissions, making it significantly more difficult to bring down emissions, resulting in higher costs with stricter emission constraints.

The range in terms of costs and emissions is summarized in the Table below. Based on this and the associated figure, it can be noted that the minimum prices (without emission constraints) can be considered economically feasible for the Nordic wood residue and the rice straw (roughly €400/tMeOH, as described in section 2.1). The interesting observation is that the extra costs, associated with stricter emission constraints, remain

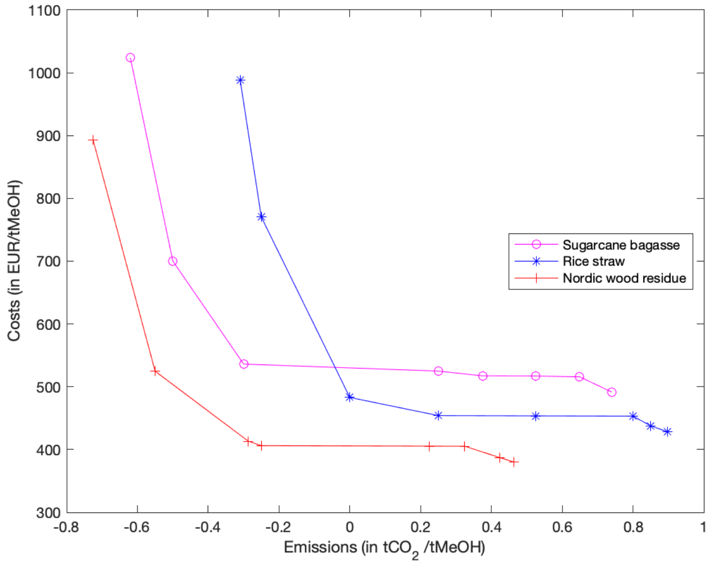

Figure 10: Pareto front displaying costs and emissions against one another for the three different biomass types. SBR as decision variable is **0.3** in all cases

relatively low up until a certain point. These rapid decreases in emissions with relatively low extra costs are caused by the deployment of a BtM plant with the capture of CO_2 in combination with an offshore carbon sink that is growing in size with stricter emission constraints. Costs are low, because the CO_2, produced during the gasification process, is already in a relatively pure form, as it has to be scrubbed out anyway, making it economically feasible to capture that scrubbed out CO_2 and utilize it by storing it underground. With that, it is even possible to obtain negative emissions of -0.3tCO_2/tMeOH with a price of €415/tMeOH for the Nordic wood residue. Finally, concerning the SBR, in all cases for each type of biomass, a SBR of 0.3 is preferred. This shows that the extra heat demand, associated with higher SBRs (>0.3), does not weigh up against the decreased biomass requirements. The impact of the SBR on the optimal design is elaborated on in section 4.2.

Table 7: Cost and emissions at extreme points for the different types of biomass

Biomass type	Cost range (€ /tMeOH)	Emission range (tCO_2/tMeOH)
Sugarcane bagasse	492 to 1015	0.77 to -0.61
Nordic wood residue	392 to 898	0.44 to -0.74
Rice straw	428 to 995	0.91 to -0.27

Technology sizing & output

As already explained briefly, the optimization of the MES results in the choice of deploying the BtM plant including the capturing and utilisation of CO_2 in combination with a carbon sink for most of the emission constraints. Only for those optimizations in which no or a minor emission constraint exist, the model decides to choose for for the BtM plant in which CO_2 is discarded, as this is the cheaper option. This is due to the fact that no investments in CO_2 compressors (for the capturing and compressing of CO_2) have to be made. Figure 11 and Figure 12 respectively show the technology sizes and output for the Nordic wood residue cases. Only the Nordic wood case is shown in this section, because of two reasons: the Nordic wood residue is the preferred type of biomass, both in terms of costs and emissions. Also, the dynamics in technology size and output do not differ much between the different types of biomass. The plots for the other types of biomass can be found in Appendix A3.

As mentioned in the paragraph above, the different biomass types show no clear differences in terms of the technology sizes and output. The main difference between the different biomass types is in the size and annual output of the carbon sink at its maximum capacity. This is explained by the fact that some biomass types (such as sugarcane bagasse) yield more CO_2 during the gasification process than other types of biomass (such as rice straw). For the biomass types assessed in this research, the explanation for that is the relatively high O% in the sugarcane bagasse, as compared to the other biomass types. Equation 9, formulated in section 3.2.1, shows that this relatively high O% in the sugarcane bagasse results in higher CO_2 contents in the synthesis gas and hence, larger capital requirements for CO_2 capture and storage are required.

Another interesting note is that in not a single situation (for neither type of biomass), the decision is made to deploy a BtM plant with the addition of hydrogen or a methanol synthesis plant in which CO_2 and H_2 are combined to produce methanol. This can be explained by two reasons. First of all, it is most likely more expensive to produce the required hydrogen for those two pathways as compared to capturing and storing the produced CO_2 in the other pathway. Next to that, the pathways including biomass have the possibility of reaching negative emissions, while the pathway of adding H_2 to the mixture or combining CO_2 and H_2 does not have the possibility of capturing and storing CO_2 during its production process. This combination of lower costs and higher potential in decreasing emissions, makes the decision to choose for a BtM plant with carbon capture and storage (with the inclusion of an offshore carbon sink) the preferred and logical choice.

Besides the deployment of the technologies for the production of methanol, this research also focuses on the deployment of the auxiliary technologies, which is also shown in Figure 10 and 11.

When assessing the deployment of heat supply technologies, it can be seen that gas boilers are preferred in situations with no emission constraints due to the lower costs for natural gas. With stricter emission constraints, electric boilers are also deployed in co-operation with gas boilers, even though grid electricity has a higher emission factor than natural gas. However, as prices for electricity vary through the day and emissions are already curbed through the deployment of carbon capture and storage, it is at some times preferred (economically speaking) to use electricity to supply for the heat; also because electric boilers have a higher conversion efficiency than gas boilers. With even stricter emission constraints and higher deployment of renewable electricity technologies, the electric boiler takes over the main supply of heat (steam) to the gasification process, as electricity becomes even more cheap and less emission intensive (due to the higher integration of renewable electricity). Hydrogen boilers are deployed at the strictest emission constraints to partly supply for the heat. This technology is simultaneously deployed with hydrogen storage, making the supply of hydrogen more economically feasible at stricter emission constraints.

Regarding renewable electricity technologies, it is found that in early stages, onshore wind turbines are deployed, while at later stages, solar PV is also added to the system. Wind turbines are preferred at earlier stages due to the weather conditions in the Netherlands that prefer wind over sun. Offshore wind turbines are not deployed in this MES yet, due to the fact that these are considered more expensive and not particularly necessary to meet the maximum emission constraints. The dynamics in the deployment of the technologies is the same for all types of biomass. For all biomass types, onshore wind is utilised within the boundaries of the available space for deployment and complemented with PV to meet the emission constraints.

Finally, regarding the deployment of energy storage and hydrogen related technologies, it can be seen that deployment of either battery storage or hydrogen storage (HOS) is only realised at extremely strict emission constraints. The electricity coming from the wind turbines and solar panels is first used to supply for the electricity and heat (via electric boilers) in the gasification and synthesis process. Only at the more extreme emission constraints, the deployment of storage technologies becomes necessary to meet the emission constraints and bring down the emissions for the methanol production process. It can be seen that hydrogen storage is significantly preferred over the battery storage, mainly due to the lower costs associated with hydrogen storage; even though hydrogen should first be produced via the use of PEMEC, typically leading to higher costs. This stored hydrogen is used to either supply for the heat directly via hydrogen boilers or to supply electricity with the use of the PEMFC running on hydrogen. Apart from absolute sizing and annual output, there are no clear differences in the technology deployment between the different biomass types.

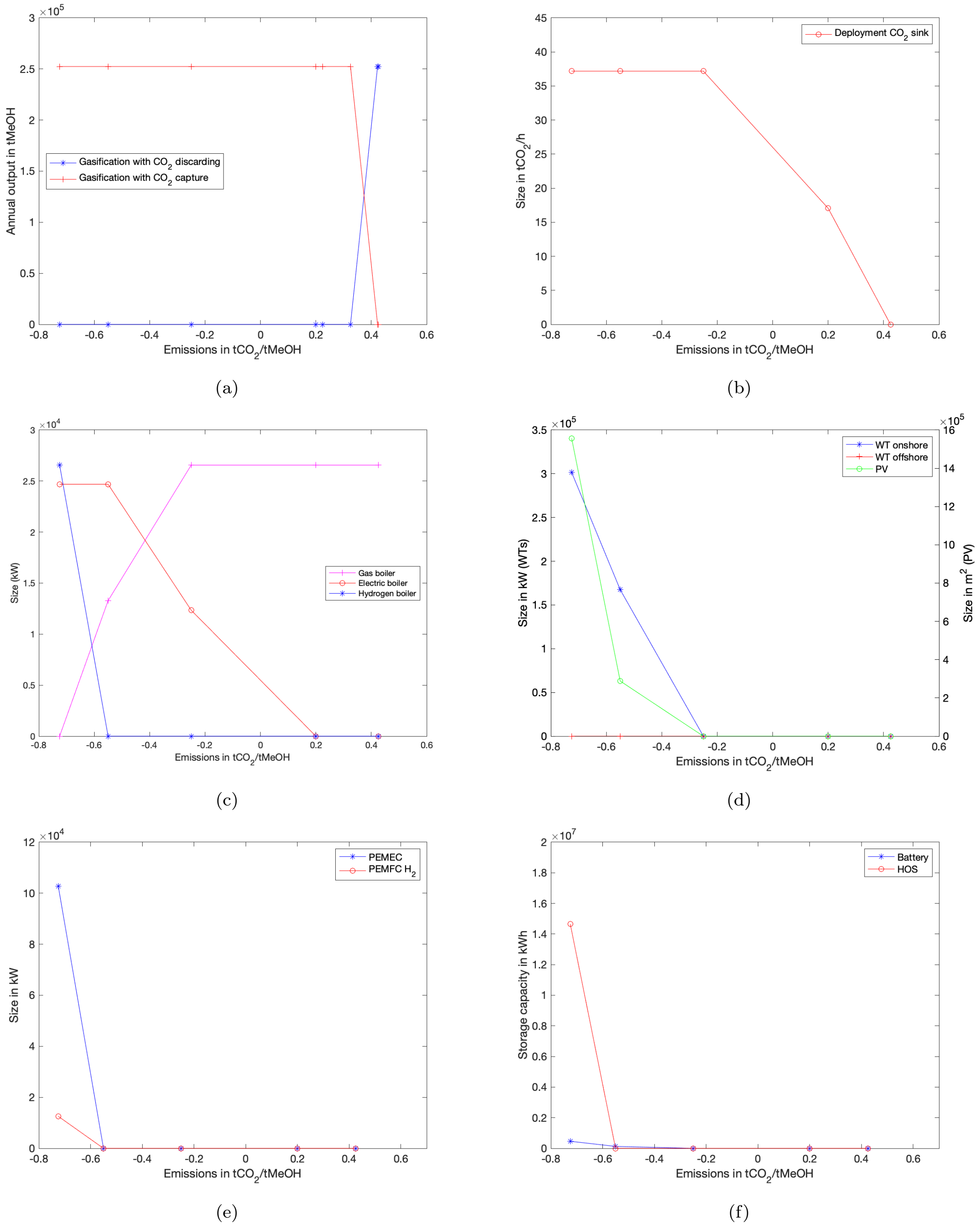

Figure 11: Technology sizes for the Nordic wood residue case with (a) displaying the technology sizes of the methanol production units, (b) displaying the size of the carbon sink, (c) displaying the boiler sizes, (d) displaying the renewable energy technology sizes, (e) displaying the sizes of the hydrogen generating and consuming technologies and (f) displaying the sizes of the storage technologies

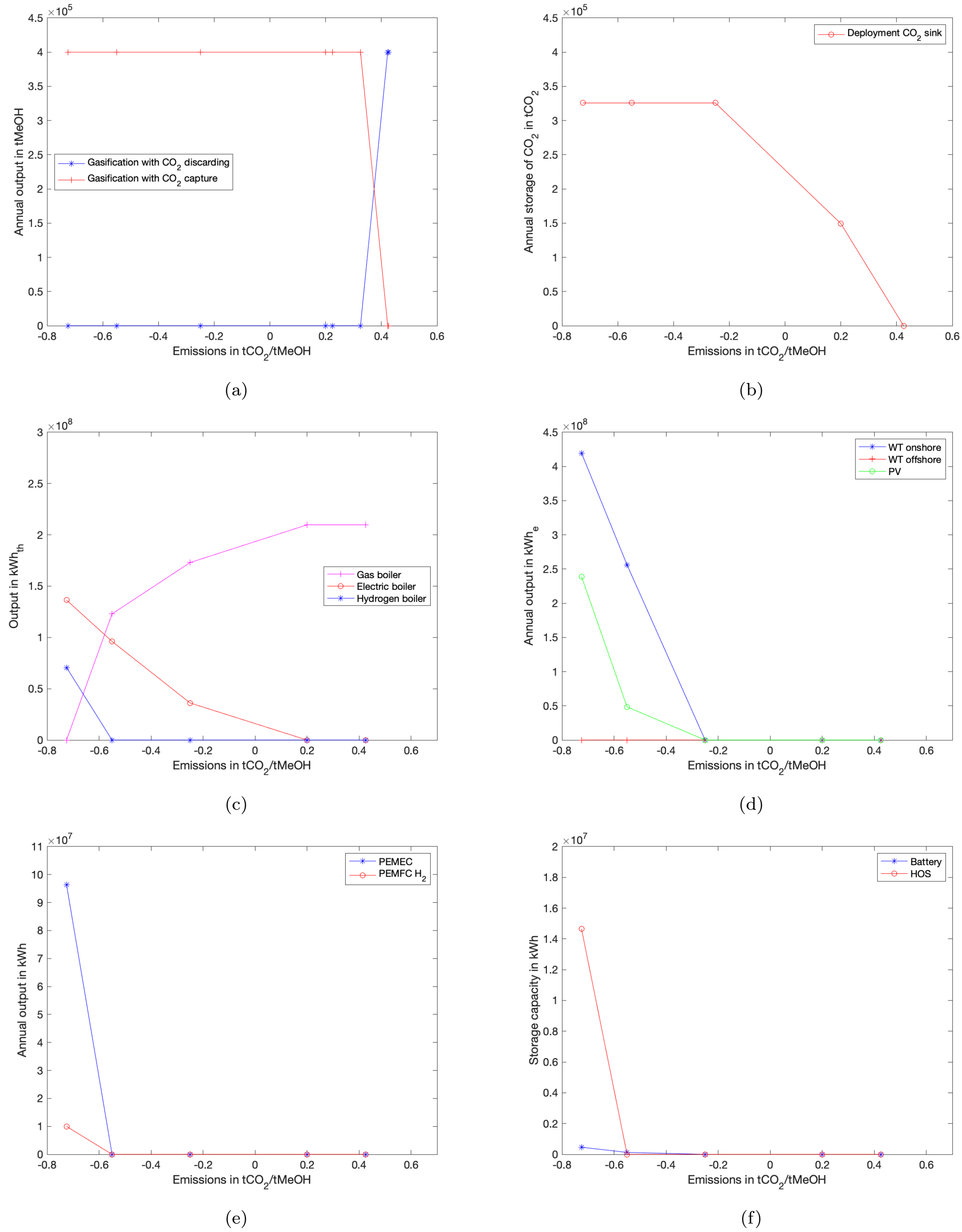

Figure 12: Annual technology outputs for the Nordic wood residue case with (a) displaying the technology outputs of the methanol production units, (b) displaying the annual storage of CO_2 in the carbon sink, (c) displaying the boiler outputs, (d) displaying the renewable energy technology outputs, (e) displaying the outputs of the hydrogen generating and consuming technologies and (f) displaying the storage sizes of the storage technologies

Technology operation

Regarding operation, it is seen that both the BtM plant and the carbon sink are operating at full capacity to meet the constant flow of demand for methanol and, if deployed, store the produced CO_2. Renewable energy technologies, such as the deployed wind turbines and solar panels show patterns, similar to the relevant weather patterns (Figure 8) for each of the technologies; solar PV peaks during sunny summer days, while wind power production flourishes during times of high wind speeds, which is mainly in the beginning and end of the year.

When looking at the boiler operation, it is seen that the gas and electric boilers are mostly co-operating. During times of low electricity prices and high integration of renewable electricity (i.e. low emissions), electric boilers are preferred and gas boilers play a back-up for situations with high electricity prices or emission factors. On the other hand, at higher electricity prices and lower integration of renewable electricity, gas boilers are preferred for the supply of heat. Hydrogen boilers only play a part when there is also a significant deployment of PEMEC and hydrogen storage (HOS) to supply for the hydrogen boiler; this is the case in the most constrained emission scenario.

Finally, an interesting result is the codependency between the production of wind and solar energy and the production (and storage) of hydrogen. In other words, during those periods of high production of solar PV and wind, PEMEC and HOS are respectively producing and charging hydrogen, while at times of low production of solar PV and wind, PEMEC and HOS are respectively stationary and discharging hydrogen. This means that it is preferred to have a flexible operation of the PEMEC to supply and or store hydrogen than to have a fixed output. An example of this is shown in Figure 13, which shows the production and storage dynamics for the Nordic wood residue case for the first 500 hours of the year, with emissions being constrained at the maximum emission constraint (i.e. -0.74 $tCO_2/tMeOH$).

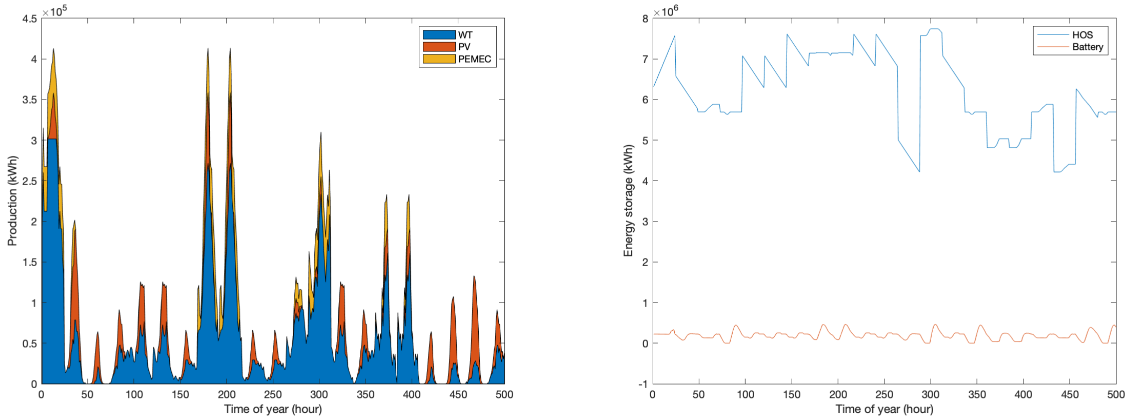

(a) (b)

Figure 13: (a) Production of solar PV, wind energy and hydrogen (PEMEC) during the first 500 hours of the year. (b) Storage dynamics for the battery and hydrogen storage components for the first 500 hours of the year. All plots are for the Nordic wood residue case at its maximum emissions constraint

To summarize, the BtM plant with CO_2 capture using Nordic wood residue is the preferred technology for the methanol production if a carbon sink is available. This carbon sink is being used in this case and increases up until its maximum size with increasing emission constraints. This configuration is preferred, because the BtM plant with CO_2 capture in combination with the carbon sink causes the methanol production costs to not increase drastically with increasing emission constraints due to the relatively low costs of both CO_2 capture and storage. This is because the CO_2, produced in the gasification process, is already in a relatively pure form, making it economically feasible to capture and eventually store it.

When comparing these results with the status quo, it is seen that although prices are higher (e.g. 325 EUR/tonne for conventional production versus 392 EUR/tonne at minimum costs using biomass gasification), its emissions can be significantly lower with only minor increases in price. Conventional production results in an average emission factor of 0.7 $tCO_2/tMeOH$ (see section 2.1), while the the results in this section show that it is possible to obtain -0.3 $tCO_2/tMeOH$ (an decrease of 1 $tCO_2/tMeOH$) for costs equal to 415 EUR/tonne.

4.1.2 Optimal design of MES without inclusion of carbon sink

The optimization of the MES without the carbon sink shows significantly different results, as can be seen in the Pareto front of Figure 14. The costs for decarbonization are significantly higher if there is no carbon sink available and the minimum emissions that can be achieved in this scenario are bound to 0. Although CO_2 from the biomass gasification process and DAC unit can lead to negative emissions, it should be permanently stored to actually be considered as negative emissions. In this scenario, however, there is no carbon sink available and hence the emission is bound at 0.

However, there are also similarities. To start, the preferred type of biomass (in terms of both emissions and costs) remains the Nordic wood residue. Both sugar cane bagasse and rice straw show economically infeasible prices starting from emissions constraints of 0.25 tCO_2/tMeOH (prices higher than €5000/tMeOH), which shows that it is incredibly difficult to fully decarbonize the methanol production process without the inclusion of a carbon sink. The extreme increase in costs at stricter emission constraints can be explained by the fact that the methanol synthesis reactor, consuming CO_2 and H_2, is being deployed. This causes both investment costs and operational costs to increase heavily. In this case, all or most of the CO_2 is provided by the BtM plant using carbon capture and utilisation, meaning that the two plants are operating in harmony of one another. At even higher emission constraints, the DAC is the main supplier of CO_2 in order to bring down the emissions coming from the biomass import. This causes the prices to skyrocket, leading to unrealistic scenarios for sustainable methanol production. Finally, the optimal SBR does not change if carbon sinks are removed from the energy system; the SBR of 0.3 remains the preferred SBR for the BtM plants. This is all visualized in the Table and figure below.

Table 8: Cost and emissions at extreme points for the different types of biomass

Biomass type	Cost range (€ /tMeOH)	Emission range (tCO_2/tMeOH)
Sugarcane bagasse	492 to 29,900	0.77 to 0
Nordic wood residue	392 to 29,870	0.44 to 0
Rice straw	428 to 30,050	0.91 to 0

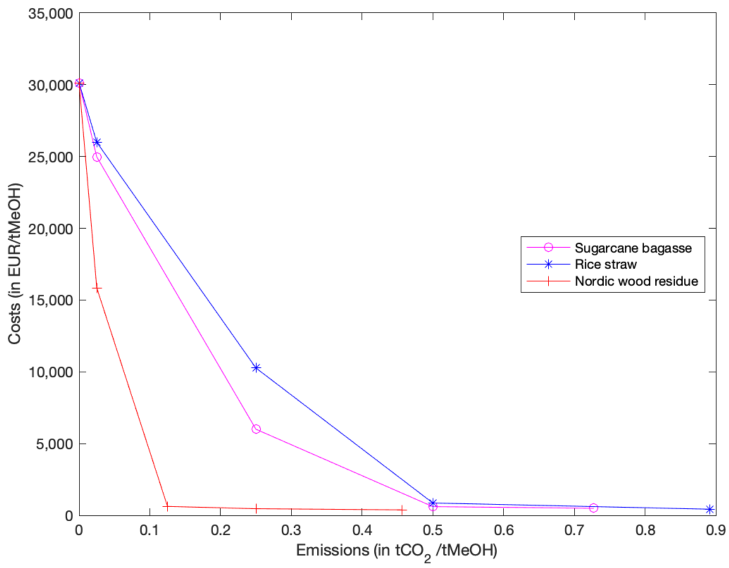

Figure 14: Pareto front displaying costs and emissions against one another for the three different biomass types. SBR as decision variable is **0.3** in all cases

Technology sizing & output

Figure 15 and 16 show the technology sizes and output for the different technologies for the Nordic wood residue case. Due to the large similarities between the different biomass types, the technology sizes and outputs of the other types of biomass are not displayed here; these can be found in Appendix A4.

As opposed to the case with a carbon sink, the BtM plant with CO_2 utilisation is not the only operating technology at stricter emission constraints. As briefly mentioned earlier, the BtM plant with CO_2 utilisation and the methanol synthesis reactor running on H_2 and CO_2 are co-operating. The CO_2 produced from the BtM plant is used as an input in the methanol synthesis reactor running on H_2 and CO_2. The reason for the inclusion of the methanol synthesis reactor running on CO_2 and H_2 can be explained by the fact that that component does not require biomass import and hence results in lower emissions. Also, the required CO_2 for the synthesis reactor has synergies with the BtM plant that captures the CO_2. As storage is no option in this scenario, the CO_2 can either be emitted or, for a relatively cheap price, be captured and utilised in the methanol synthesis reactor. Only at extreme emission constraints, the BtM plant is completely removed and the required CO_2 comes from the DAC. This is done in order to remove the emissions from the biomass import, associated with the BtM plant. Differences between the biomass types exist, but are minor. The Nordic wood residue prefers the BtM plant with CO_2 discarding over other methanol plants, even when emission constraints become more stringent. This can be explained by the fact that the import of Nordic wood residue leads to only low emissions from biomass import (due to low transport emissions). This leads to the fact that it only becomes necessary to replace BtM plants with cleaner methanol production technologies (i.e. methanol synthesis reactor using CO_2 and H_2 and BtM plants with CO_2 capture) at more stringent emission constraints.

Regarding the technologies for the supply of heat, it is found that, as in the case with the carbon sink, electric boilers become more present at stricter emission constraints. The increase in the use of electric boilers is even increasing faster at stricter emission constraints, most likely due to the simultaneous deployment of wind turbines and solar PV, making the use of electricity cheaper and less emission intensive. Hydrogen boilers are, just as in the case including the carbon sink, preferred only in the final stages, due to the possibility of storing hydrogen for cheaper prices than electricity. The sudden divergence in size of the boilers is explained by the fact that the DAC is deployed at stricter emission constraints. As the DAC is consuming significant amounts of heat, boiler capacity needs to be increased.

Renewable energy deployment and output follows the same trajectory as the renewable energy deployment and output in the case with a carbon sink. The main difference is the increasingly larger sizes and outputs. In this scenario, offshore turbines are also deployed, but only at the strictest emission constraints, due to their high prices. Offshore turbines are deployed, because the onshore turbines are bound to area constraints and reach the maximum capacity that can be installed at those stricter emissions constraints. The reason for the larger deployment of renewable energy technologies lies in the fact that there is a simultaneous deployment of the methanol synthesis reactor using CO_2 and H_2 as well as a deployment of the DAC. Of these technologies, the first consumes significant amounts of hydrogen, while the latter consumes both electricity and heat. To supply for this and meet emission constraints, a larger deployment of wind turbines and solar PV is required. Differences in the deployment of boilers and renewable energy technologies differ slightly between the biomass types and are mainly explained by the larger emissions associated with each biomass type. This, for example, leads to a faster and larger deployment of respectively the electric boiler and renewable energy technologies for the rice straw case if emission constraints become stricter, as this is required to bring down emissions and meet emission constraints.

Finally, the deployment of energy storage and hydrogen production technologies is assessed. The deployment of battery and hydrogen storage looks similar to the case with the inclusion of a carbon sink; hydrogen storage is preferred over battery storage, most likely due to the lower costs associated with hydrogen storage. The main difference is the size; the HOS reaches its theoretical maximum of 10 GWh for all types of biomass. This is explained by the fact that a lot of processes consume hydrogen. At the strictest emission constraint, heat is supplied by hydrogen boilers and pure hydrogen is consumed in combination with CO_2 to produce methanol in the methanol synthesis reactor. This can also be seen in the deployment of PEMEC, which roughly follows the same trajectory as the deployment of the HOS. The main difference between the two cases is the absence of a PEMFC. This is most likely due to the significantly higher hydrogen consumption in the case without a carbon sink than the case with a carbon sink, making the deployment of a PEMFC rather redundant.

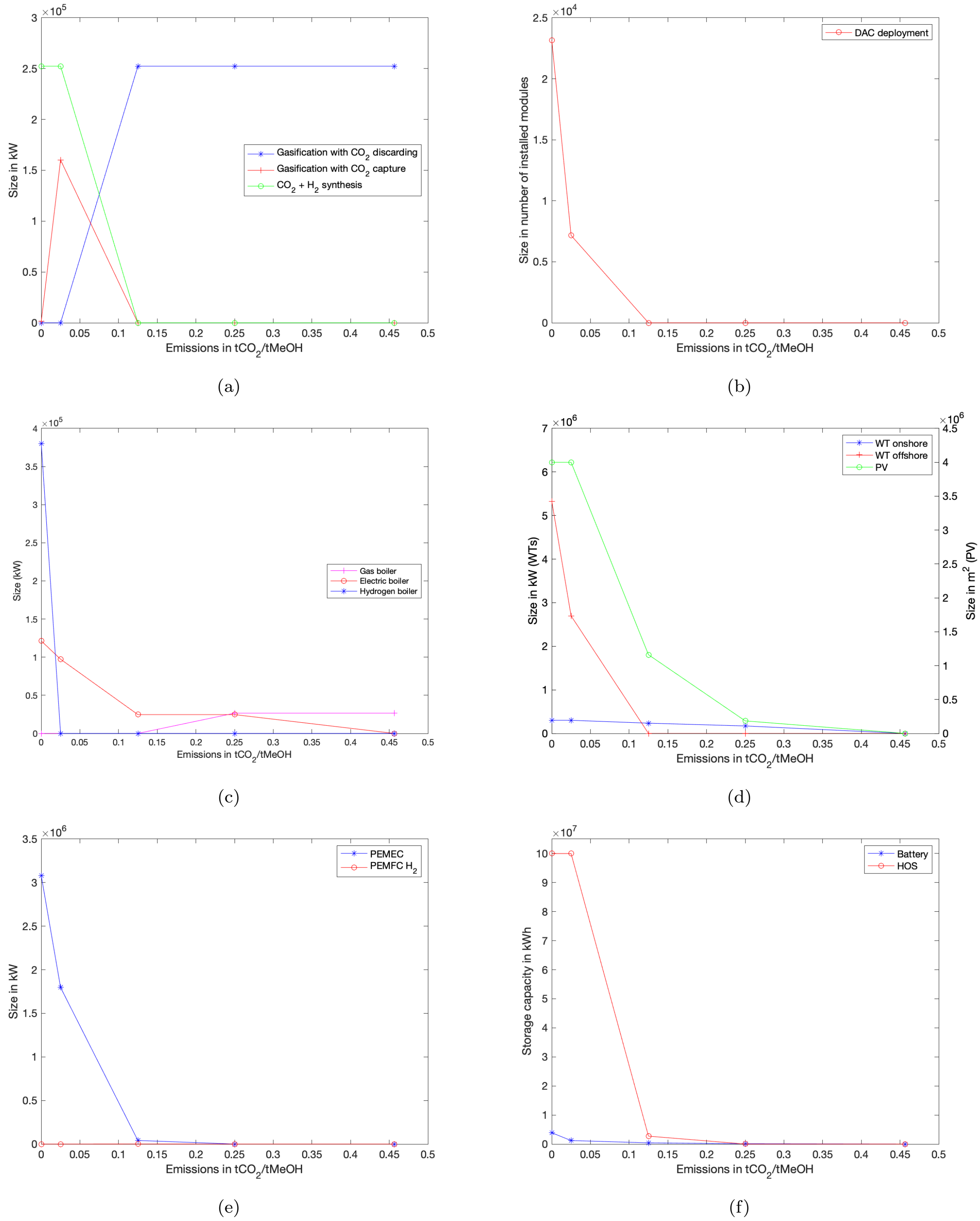

Figure 15: Technology sizes for the Nordic wood residue case with (a) displaying the technology sizes of the methanol production units, (b) displaying the size of the DAC, (c) displaying the boiler sizes, (d) displaying the renewable energy technology sizes, (e) displaying the sizes of the hydrogen generating and consuming technologies and (f) displaying the sizes of the storage technologies

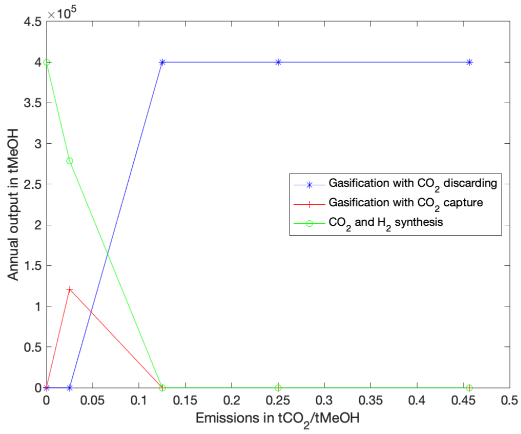

(a)

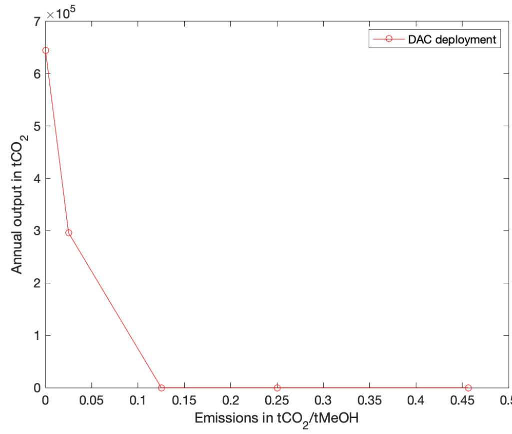

(b)

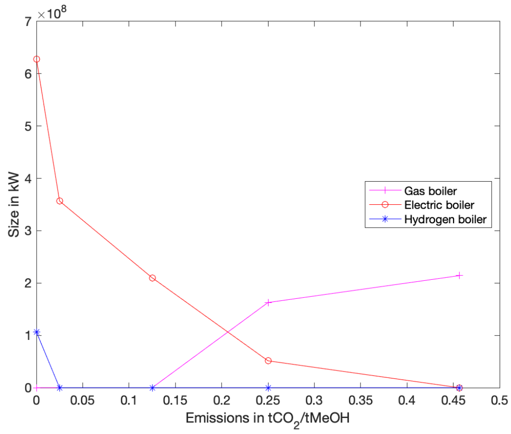

(c)

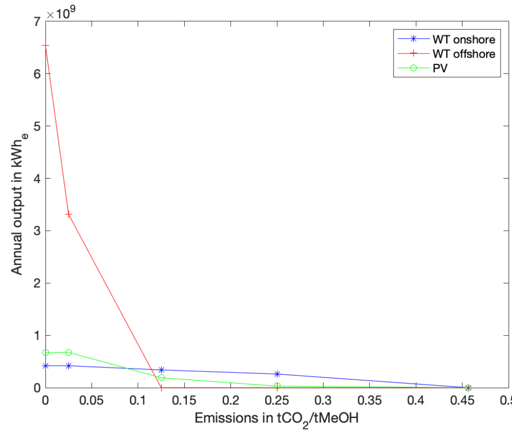

(d)

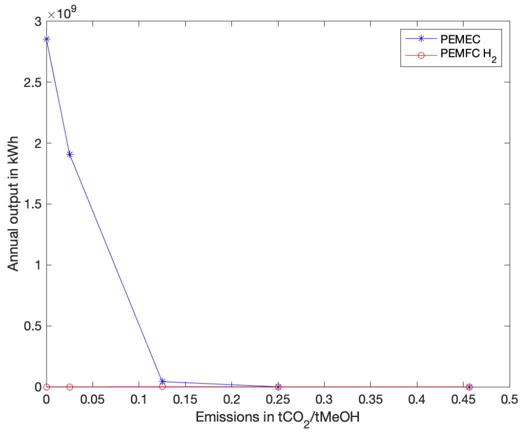

(e)

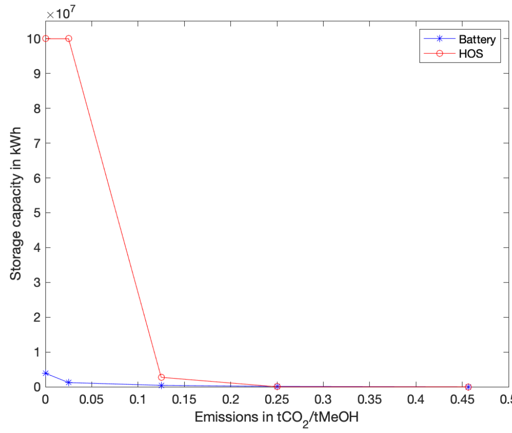

(f)

Figure 16: Annual technology outputs for the Nordic wood residue case with (a) displaying the technology outputs of the methanol production units, (b) displaying the annual production of CO_2 in the DAC, (c) displaying the boiler outputs, (d) displaying the renewable energy technology outputs, (e) displaying the outputs of the hydrogen generating and consuming technologies and (f) displaying the storage sizes of the storage technologies

Technology operation

As is also seen in the case with a carbon sink, the technologies for the production of methanol mainly run in a steady operation. At stricter emission constraints, the technologies are co-operating with one another in a steady operation to supply for the methanol. Regarding the operation of the boilers, it is seen that, as in the other case, gas boilers dominate until electricity prices and emission factors decrease due to the higher integration of renewable electricity. Only at the strictest emission constraint, hydrogen boilers take over, as renewable hydrogen supply becomes preferred due to the relative cheap storage of hydrogen as compared to the storage of electricity. Finally, the operation of the PEMEC is again codependent on the production of renewable electricity, meaning that hydrogen is predominantly produced and stored in times of high wind and solar PV production.

To summarize, a scenario without the inclusion of a carbon sink seems highly unlikely. Prices surge, while emissions do not go down as quickly as in the case with carbon sink. This is because negative emissions, normally coming from the biomass, cannot be reached in this scenario. This means that investments in expensive renewable energy technologies have to be made to bring down the emissions. In that sense, it is preferred to either not go for a scenario without a carbon sink or to deploy a BtM plant without carbon capture with the use of Nordic wood residue. It is not preferred to deploy a methanol synthesis reactor running on CO_2 and H_2 as this requires significant investments in PEMEC (and HOS) to supply for the H_2. This would only be preferred if emissions constraints are really stringent and no carbon sink is available. Investments in electric boilers and renewable energy technologies can be made and can bring down emissions up until 0.15 tCO_2/tMeOH, while keeping the cost increases relatively limited (750 EUR/tMeOH). When, however, comparing this to the status quo, it can be clearly seen that it is not preferable to go via this pathway. Emissions are only reduced by 0.55 tCO_2/tMeOH, while prices increase with more than 400 EUR/tMeOH.

4.2 Impact of SBR on optimal design of MES

As the previous paragraph has clearly shown that Nordic wood residue is the preferred biomass type, the impact of the SBR on the optimal design and operation of the MES is assessed based on this biomass type. Figure 17 shows the impact of the assessed SBRs on the cost and emissions of the optimal design configuration. In these figures it can be seen that an increasing SBR typically results in higher costs and emissions, both for the cases with and without a carbon sink. This goes to show that the extra heat demand with higher SBRs does not weigh up against the decreased biomass demand. This can mainly be explained by the fact that, besides the extra requirement for energy carriers (such as heat, gas or electricity), to supply for the extra heat demand, there is also an extra requirement in the deployment of heat production technologies, causing the costs to go up quite significantly. This then also translates in larger sizes for hydrogen and electricity storage a stricter emission constraints, increasing the costs even more.

When assessing the choice of technology for the production of methanol, no differences (apart from sizes and output) are found between the different SBRs. In the case with a carbon sink, the choice quickly shifts to a BtM plant with CCUS with increasing emission constraints. Meanwhile, in the case without a carbon sink, the choice moves to a situation where a BtM plant with CCU and a methanol synthesis reactor using CO_2 and H_2 are co-operating in harmony, after which the latter becomes the dominant technology, when emissions are a the strictest constraint.

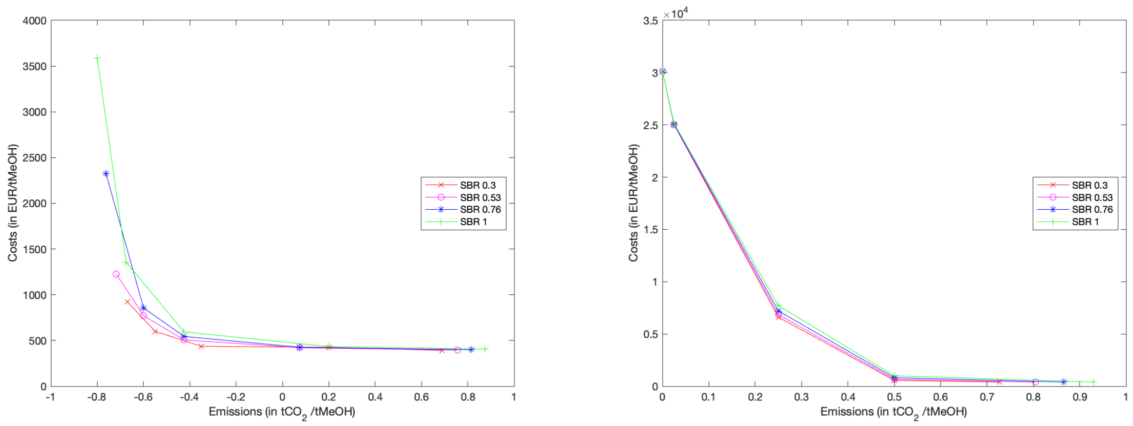

(a) (b)

Figure 17: Impact of SBR on the costs and emissions of the optimal design configuration with (a) showing the Pareto fronts for the scenario including a carbon sink and (b) showing the Pareto fronts for the scenario excluding a carbon sink (right)

4.3 Sensitivity analysis

As mentioned in section 3.3.3, a sensitivity analysis is performed on the biomass prices and methanol output, using a scenario approach. In this approach there are four different scenarios for the two main cases (including and excluding a carbon sink). In these scenarios the prices for biomass are either in- or decreased by 30%, as mentioned in Duic et al., [16], while simultaneously the hourly methanol demand is in- or decreased by 50%. The scenario analyses are performed for the preferred type of biomass: the Nordic wood residue. The different scenarios are summarized in the table below.

Table 9: Scenarios assessed in sensitivity analysis

	Price down	Price up
Demand down	S1	S2
Demand up	S3	S4

The Pareto fronts for the different scenarios are shown in Figure 18. Based on this, it can be seen that S3 results in the lowest overall methanol production costs for most of the emission constraints. This makes sense, as low biomass prices result in lower operational costs, while at the same time larger demands lead to economies of scale in production, causing further reductions in costs. Only for the most extreme emission constraints, the higher demand figures are less preferred in terms of costs. This can be explained by the fact that increasingly larger capacities of renewable energy technologies and storage technologies are required to meet the emission constraints at higher methanol demand figures as compared to situations with lower demand. This increase is exponential in this case as there are area constraints for the production of onshore wind and solar energy, meaning that extra investments in energy storage and offshore wind energy is required at higher demand figures. This leads to extra unit investment costs, making economies of scale in this case irrelevant.

When assessing the technology deployment and operation, no significant changes are seen. For the case including the carbon sink, the BtM plant in which CO_2 is discarded is quickly replaced by the BtM plant using CCU(S) if emission constraints become more stringent. This goes hand in hand with the deployment of a carbon sink and at more stringent constraints, the deployment of renewable energy technologies and storage technologies.

For the case excluding the carbon sink, the simultaneous deployment of the BtM plant with CCU and the $CO_2 + H_2$ synthesis reactor can be seen at more stringent emission constraints. There is no difference in optimal SBR between the different scenarios. Just as in the results shown in section 4.1.1 and 4.1.2, the optimal SBR remains 0.3.

The main difference is that the deployment of these two technologies in the case without carbon sink already takes place at less stringent emission constraints, when biomass prices are increased. This makes sense, as it becomes economically more attractive to replace biomass consuming technologies with technologies consuming other energy carriers (such as CO_2 and H_2) when emission constraints become more stringent. Apart from choice, it makes sense that the sizes and outputs of both the methanol production plants, as well as the auxiliary technologies, are significantly higher for the the scenarios with increased methanol demand than for those with decreased methanol.

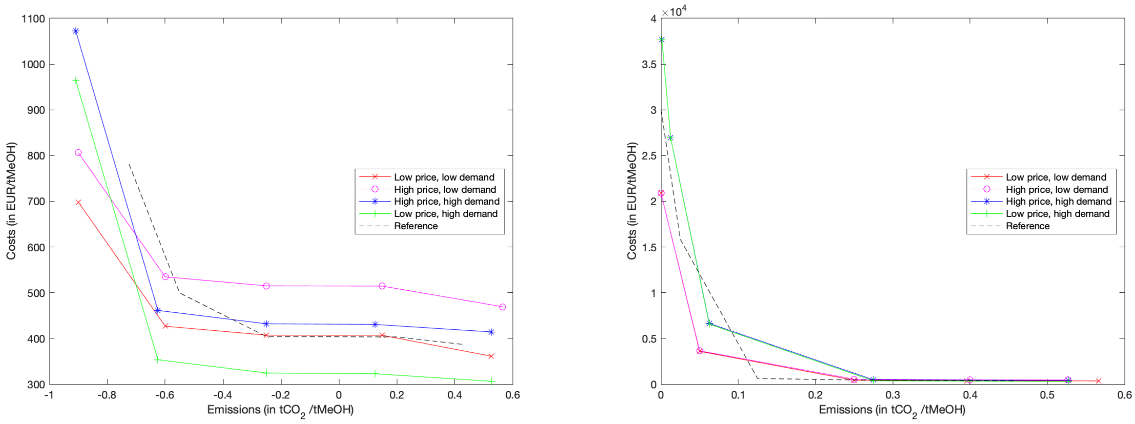

(a) (b)

Figure 18: Pareto plots for sensitivity analysis with higher and lower methanol demand and biomass prices for the two main cases with (a) showing the results for the case with carbon sink and (b) showing the results for the case without a carbon sink.

5 Discussion

In this section, the results and used methods are discussed. The limitations of the research and associated model are presented and the obtained results are compared to similar studies. Finally, recommendations for further research are provided.

Discussion of methods and results

The previous chapter shows that there are significant differences in the optimal design of a MES for the production of low-carbon methanol between the cases with and without a carbon sink. Differences are also found between the different biomass types. Biomass types from close by (e.g. Nordic wood residue) score significantly better than biomass types that come from more distant places (e.g. Indonesian rice straw). Differences are found in both costs, emissions, with the case including a carbon sink scoring significantly better in both costs and emissions. The determined optimal designs in both the case with and without carbon sink are bound to several assumptions. These assumptions could potentially have a big impact on the final result and should therefore be discussed.

One limitation is related to the assumption that is used to determine the biomass emissions. In this research, the assumption is made that all emissions in the use of biomass lie in the transport from port to port. A different approach in which, for example, a more extensive research in the gate-to-gate emissions of the associated biomass is taken into account (e.g. land transport, harvesting), the emission factor would most likely increase for all types of biomass. On the other hand, it would also be possible to set emissions for biomass completely to 0. In such a case, gate-to-gate emissions are completely left out. In the first scenario, it would become increasingly difficult to bring down emissions from the gasification process. This could potentially lead to increased costs with more stringent emission constraints. In the latter scenario, it actually becomes easier to bring down emissions. The results would most likely indicate cheaper prices at the same emission constraints.

Another limitation in this research lies within the data collection and specification of the parameters for the gasification process (KPIs). To determine the KPIs (i.e. electricity, heat, hydrogen and biomass consumption per kWh of methanol), this research uses knowledge from predictive steam gasification models by Sreejith et al., (2012) and Sreejith et al., (2014) [54] [55] to determine synthesis gas compositions and outputs, which is then combined with methanol synthesis gas requirements (composition & quantities) to establish the required amounts of biomass, steam, electricity and, in some cases, hydrogen for the production of one unit of methanol. In this process, assumptions and simplifications are made to make sure that the inputs fits properly with the research design and model used in this research. To determine the biomass consumption in the gasification process, for example, it was assumed that the hydrogen demand in the synthesis gas would need to be satisfied, while the excess CO_2 could be scrubbed out. In this scenario it was assumed that the excess CO, albeit only in small quantities, was discarded. In reality, it would change the R-ratio (equation 1, section 2.2), leading to a lower productivity and hence lower methanol output. The same can be said for the recycling of steam and heat in the gasification process. In this research, it is assumed that the steam is consumed and no excess steam or heat can be reused, while in reality, recycling of excess heat production is a common practice to improve the overall system efficiency. This would have the consequence that the heat consumption for each SBR mode would change, potentially leading to different outcomes in terms of the optimal SBR for biomass gasification.

The reason for all of these considerations to not be implemented in the tool is predominantly related to the uncertainties associated with it. The implementation of these considerations in the tool would lead to the use of even more assumptions and hence the possibility of less accurate results, as correct implementation is difficult to achieve. However, a proper assumption regarding these considerations would make the results more robust and hence reliable.

Comparison

One of the key results in this research is the fact that negative emissions can be reached with relatively small increases in production costs. To compare this with other studies, a reference is made to a paper on the global costs of carbon capture and storage by Irlam et al., (2017) [33]. Irlam et al., (2017) mentions that 'facilities with low cost increases for CO_2 capture already produce concentrated CO_2 streams as part of the process'. For biomass to fuel systems, CO_2 avoided costs average around 26.5 US$/t$CO_2$. In this research it was found that costs for biomass gasification systems using Nordic wood residue only increase by 23 EUR/tMeOH (392 EUR/tMeOH to 415 EUR/tMeOH) with emissions going down from 0.44 tCO_2/tMeOH to -0.3 tCO_2/tMeOH, purely through the addition of a carbon sink. Although this is not a decrease of 1 tCO_2/tMeOH, hence making it hard to compare the two, it still shows that the capture and storage costs, mentioned in the paper by Irlam et al., (2017) [33], are in a similar range as the ones found in this research.

Another similar study, focusing on the optimal SBR on the other hand, found different results than the ones obtained in this research. Puig-Gamero et al., (2018) mentions an optimal SBR of 0.9 for the production of methanol from biomass gasification in similar gasification conditions, as this would yield the best conditions (in terms of the ratio between H_2 and CO_2) to produce methanol. So, from a technical point of view, it would be preferred to have a higher SBR than the one shown in this research: a SBR of 0.3. However, the research from Puig-Gamero et al., (2018) did not focus on the overall system design for the production of methanol, including its auxiliary technologies, such as boilers, and electricity supply technologies. The analysis performed in this research did focus on the inclusion of auxiliary technologies and found that the extra heat consumption, and hence extra investments in heat production (and storage) technologies, does not weigh up against the lower biomass consumption, associated with the higher SBRs.

Relevance

These comparisons show the relevance of this research. Although high SBRs are preferred for technical reasons, this paper shows that lower SBRs are more preferred, when assessing overall system designs. With that statement, this research contributes to the earlier mentioned needs of Bozzano et al., (2016) [8], who urges the need of overall system optimizations for methanol production. In a low-carbon methanol production system, it is shown that low SBRs, biomass from close by and CO_2 storage are the main components to effectively produce methanol; both from a cost- as well as an emission perspective.

From a more societal point of view, this research shows that reducing carbon emissions in the industrial cluster of Rotterdam is possible with the implementation of biomass gasification systems including carbon capture and storage. With one of the scenarios, in which the industrial cluster intends to become a major biomass hub, together with the development of the CO_2 storage project (Porthos Project), Rotterdam is on a good pathway to reduce carbon emissions. Although the input data in this research focused on the Rotterdam case, and results are therefore not useful for different cases, it does show that biomass energy products with the inclusion of carbon storage have the potential of reducing carbon emissions with relatively low extra costs. It is therefore recommended for other industrial clusters that aim on becoming a large player in the production of synthetic fuels, to also take this into account.

Recommendations for further research

The main recommendation for further research would be to include two extra considerations in the multi-energy system approach: (i) conventional methanol production and (ii) carbon taxes. As this research shows that reaching zero or negative emissions is possible for relatively low extra costs, it would be interesting to see at what carbon price the production of methanol from renewable sources (such as biomass) becomes more attractive (in terms of costs) than the conventional method. If the results of such a study would be positive and a relatively low carbon price would already yield good results in terms of costs, the implementation of biomass gasification systems for the production of methanol (or other synthetic fuels) would become even more interesting to not only bring down emissions, but also overall system costs.

6 Conclusion

This research assessed multiple configurations of MES for the production of methanol in the industrial cluster of Rotterdam. The goal with this assessment is to find the optimal design and operation of such a MES.

It is found that configurations that include a carbon storage facility are preferred over cases that do not. Biomass gasification with carbon capture and storage is the preferred technical configuration at most emission constraints in that case and is capable of reaching negative emissions (-0.3tCO_2/tMeOH) for prices as low as 415 EUR/tMeOH for the cheapest type of biomass (i.e. Nordic wood residue). This is due to the fact that the CO_2, produced in the gasification process, is already in a relatively pure form, making it easy to capture and eventually store it. Although exact prices and associated emissions are hard to determine due to assumptions being made, the main results in this research do give an indication on the estimated costs and emissions and show that low-carbon methanol production is possible for reasonable prices. The case without a carbon sink shows that it is extremely difficult to reduce emissions without a carbon sink. The large investments in expensive renewable energy (storage) technologies, used to bring down emissions, cause the costs to increase to such an extent that these configurations are not preferred for deployment yet.

Furthermore, differing the biomass type does not change much to the dynamics in the deployment of (auxiliary) technologies to produce methanol; there are also only minor differences in the KPIs for the production of methanol among the different types of biomass. The different biomass types do however significantly impact the costs and emissions associated with the different cases, as emissions and costs associated with biomass are different. Typically, biomass resources from locations close by are preferred due to their low emissions and costs for transport. The low emissions should however be nuanced by the fact that the biomass emissions are purely focused on the emissions from sea transport; more adequate estimations of emission factors or no biomass emission factors at all, could influence this result. In this research, however, the Nordic wood residue is the preferred type of biomass. The other types of biomass, coming from locations far outside of Europe (South-America and Asia), increase costs with roughly 100 EUR/tMeOH to ensure the same, negative emissions.

Moreover, the SBR does not significantly impact the optimal design; lower SBRs generally lead to better results in terms of costs and emissions; the lower demand for biomass does not weigh up against the increased demand for heat (both in terms of costs and emissions). Finally, the sensitivity analysis shows that biomass prices and methanol demand have an impact on the costs and emissions associated with the optimal design of the MES. Increased methanol demand with lower biomass prices can drastically reduce costs at same emission constraints; only at the most stringent emission constraints, lower methanol demand is preferred in terms of costs, due to the lower investments in expensive renewable energy (storage) technologies.

For the industrial cluster of Rotterdam, it is recommended to pursue their ambitions of becoming a major biomass hub. The production of biomass based methanol with the inclusion of carbon capture (in the gasification process) and subsequent storage could have a significant impact on reducing their current carbon emissions and could therewith contribute to the decarbonization activities currently in place in the industrial cluster.

7 References

References

[1] A. AlNouss, G. McKay, and T. Al-Ansari. A techno-economic-environmental study evaluating the potential of oxygen-steam biomass gasification for the generation of value-added products. *Energy Conversion and Management*, 196(January):664–676, 2019.

[2] B. Anicic, P. Trop, and D. Goricanec. Comparison between two methods of methanol production from carbon dioxide. *Energy*, 77:279–289, 2014.

[3] M. Anshar, F.N. Ani, and A.S. Kader. Potential Surplus of Rice Straw as a Source of Energy for Rural Communities in Indonesia. *Applied Mechanics and Materials*, 695(November 2015):806–810, 2014.

[4] José M. Arroyo and Antonio J. Conejo. Modeling of start-up and shut-down power trajectories of thermal units. *IEEE Transactions on Power Systems*, 19(3):1562–1568, 2004.

[5] T. Blumberg, T. Morosuk, and G. Tsatsaronis. Exergy-based evaluation of methanol production from natural gas with CO2 utilization. *Energy*, 141:2528–2539, 2017.

[6] M.J. Bos, S.R.A. Kersten, and D.W.F. Brilman. Wind power to methanol: Renewable methanol production using electricity, electrolysis of water and CO2 air capture. *Applied Energy*, 264(February):114672, 2020.

[7] S. Boschma, I. Kees, and W. Kwant. Netherlands Programmes Sustainable Biomass. Technical Report June, 2013.

[8] G. Bozzano and F. Manenti. Efficient methanol synthesis: Perspectives, technologies and optimization strategies. *Progress in Energy and Combustion Science*, 56:71–105, 2016.

[9] E. Burridge. European chemical profile: Methanol. https://www.icis.com/explore/resources/news/2009/11/16/9263011/european-chemical-profile-methanol, 2009.

[10] Gabriele Calì, Paolo Deiana, Claudia Bassano, Simone Meloni, Enrico Maggio, Michele Mascia, and Alberto Pettinau. Syngas production, clean-up and wastewater management in a demo-scale fixed-bed updraft biomass gasification unit. *Energies*, 13(10), 2020.

[11] CBS. Rendement en CO2-emissie elektriciteitsproductie 2019. https://www.cbs.nl/nl-nl/maatwerk/2020/08/rendement-en-co2-emissie-elekrtriciteitproductie-2018, 2019.

[12] CBS. Aardgas & electriciteit: gemiddelde prijzen van eindverbruikers. https://opendata.cbs.nl/#/CBS/nl/dataset/81309NED/table, 2020.

[13] L.R. Clausen, N. Houbak, and B. Elmegaard. Technoeconomic analysis of a methanol plant based on gasification of biomass and electrolysis of water. *Energy*, 35(5):2338–2347, 2010.

[14] F. Dalena, A. Senatore, A. Marino, A. Gordano, M. Basile, and A. & Basile. Methanol production and applications: An overview. *Methanol*, pages 3–28, 2018.

[15] R Detz. Methanol production from CO2: Technology Factsheet, 2019.

[16] N. Duić, N. Štefanić, Z. Lulić, G. Krajačić, T. Pukšec, and T. Novosel. EU28 fuel prices for 2015, 2030 and 2050. *Heat Roadman Europe 2050*, (695989), 2017.

[17] EEA. *Europe's onshore and offshore wind energy potential*. Number 6. 2009.

[18] W. Elbersen and R. Diaz-Chavez. Towards a Sustainable European Bioenergy Trade Strategy for 2020 and beyond. A case study: Biomass export potential of Colombia. 2016.

[19] ENTSO-E. Day-ahead electricity prices Netherlands. https://transparency.entsoe.eu/transmission-domain/r2/dayAheadPrices/show, 2019.

[20] E. Fabrizio, V. Corrado, and M. Filippi. A model to design and optimize multi-energy systems in buildings at the design concept stage. *Renewable Energy*, 35(3):644–655, 2010.

[21] H. Firmansyah, Y. Tan, and J. Yan. Power and methanol production from biomass combined with solar and wind energy: Analysis and comparison. *Energy Procedia*, 145:576–581, 2018.

[22] P. Gabrielli, F. Fürer, G. Mavromatidis, and M. Mazzotti. Robust and optimal design of multi-energy systems with seasonal storage through uncertainty analysis. *Applied Energy*, 238(December 2018):1192–1210, 2019.

[23] P. Gabrielli, M. Gazzani, E. Martelli, and M. Mazzotti. Optimal design of multi-energy systems with seasonal storage. *Applied Energy*, 219:408–424, 2018.

[24] P. Gabrielli, M. Gazzani, and M. Mazzotti. Electrochemical conversion technologies for optimal design of decentralized multi-energy systems: Modeling framework and technology assessment. *Applied Energy*, 221:557–575, 2018.

[25] M. Geidl, G. Koeppel, and P. Favre-Perrod. The Energy Hub: A powerful concept for future energy systems. (March):13–14, 2007.

[26] F. Glover. Improved Linear Integer Programming Formulations of Nonlinear Integer Problems. 22(4):455–460, 1975.

[27] Gurobi. Mixed-Integer Programming (MIP) - A Primer on the Basics Branch-and-Bound. http://www.gurobi.com/resources/getting-started/mip-basics [Online accessed on 24th of November 2020], 2020.

[28] I. Hannula and E. Kurkela. *Liquid transportation fuels via large-scale fluidised-bed gasification of lignocellulosic biomass*. 2013.

[29] J.M. Helseth. Biomass with CO2 capture and storage (Bio-CCS): The way forward for europe. *Industrial Biotechnology*, 8(4):182–188, 2012.

[30] K.M. Holmgren, T. S. Berntsson, E. Andersson, and T. Rydberg. Perspectives on investment cost estimates for gasification-based biofuel production systems. *Chemical Engineering Transactions*, 45(1):427–432, 2015.

[31] G. H. Huisman, G. L.M.A. Van Rens, H. De Lathouder, and R. L. Cornelissen. Cost estimation of biomass-to-fuel plants producing methanol, dimethylether or hydrogen. *Biomass and Bioenergy*, 35(SUPPL. 1):S155–S166, 2011.

[32] A. Ingham. Reducing the carbon intensity of methanol for use as a transport fuel. *Johnson Matthey Technology Review*, 61(4):297–307, 2017.

[33] L. Irlam. Global Costs of Carbon Capture and Storage. *Global CCS Institute*, (June), 2017.

[34] P. Jie, F. Wei, F. Zhang, and J. Li. Evaluating the performance of biomass gasification based combined cooling, heating, and power system operated under different operating strategies. *Advances in Mechanical Engineering*, 11(2):1–17, 2019.

[35] M. Khandelwal and T. van Dril. Decarbonisation options for the Dutch biofuels industry | PBL Planbureau voor de Leefomgeving. *The Hague, 2020, PBL publication number: 3887*, (April):67, 2020.

[36] KNMI. KNMI - Uurgegevens van het weer in Nederland. https://www.knmi.nl/nederland-nu/klimatologie/uurgegevens [Online accessed on 24th of November 2020], 2020.

[37] D. S. Kourkoumpas, E. Papadimou, K. Atsonios, S. Karellas, P. Grammelis, and E. Kakaras. Implementation of the Power to Methanol concept by using CO2 from lignite power plants: Techno-economic investigation. *International Journal of Hydrogen Energy*, 41(38):16674–16687, 2016.

[38] C.F.R. Machado, J.L. Medeiros, O.F.Q. Araújo, and R.M.B. Alves. A comparative analysis of methanol production routes : synthesis gas versus CO2 hydrogenation. *2014 International Conference on Industrial Engineering and Operations Management*, pages 2981–2990, 2014.

[39] P. Mancarella. MES (multi-energy systems): An overview of concepts and evaluation models. *Energy*, 65:1–17, 2014.

[40] S. Meulen, T. Grijspaardt, W. Mars, W. Geest, and A.R. Kiel. Cost Figures for Freight Transport: Final report, 2020.

[41] A. Molino, V. Larocca, S. Chianese, and D. Musmarra. Biofuels production by biomass gasification: A review. *Energies*, 11(4):1–31, 2018.

[42] I.L. Motta, N.T. Miranda, R. Maciel Filho, and M.R. Wolf Maciel. Sugarcane bagasse gasification: Simulation and analysis of different operating parameters, fluidizing media, and gasifier types. *Biomass and Bioenergy*, 122(February):433–445, 2019.

[43] Port of Rotterdam. The power of Wind Energy in the Port of Rotterdam. 2016.

[44] L.P.R. Pala, Q. Wang, G. Kolb, and V. Hessel. Steam gasification of biomass with subsequent syngas adjustment using shift reaction for syngas production: An Aspen Plus model. *Renewable Energy*, 101:484–492, 2017.

[45] Port Rotterdam. European Hub for Biomass. https://www.portofrotterdam.com/sites/default/files/european-hup-for-biomass-port-of-rotterdam.pdf?token=hpNVWJXR, 2020.

[46] Port Rotterdam. Rotterdam Energy Port. https://www.portofrotterdam.com/sites/default/files/ Rotterdam-Energy-Port.pdf?token=g3v0nAnF, 2020.

[47] M. Puig-Gamero, J. Argudo-Santamaria, J. L. Valverde, P. Sánchez, and L. Sanchez-Silva. Three integrated process simulation using aspen plus®: Pine gasification, syngas cleaning and methanol synthesis. *Energy Conversion and Management*, 177(October):416–427, 2018.

[48] M.L.G. Renó, E.E.S. Lora, J.S.C. Palacio, O.J. Venturini, J. Buchgeister, and O. Almazan. A LCA (life cycle assessment) of the methanol production from sugarcane bagasse. *Energy*, 36(6):3716–3726, 2011.

[49] A.M. Ribeiro, J.C. Santos, A.E. Rodrigues, and S. Rifflart. Syngas Stoichiometric Adjustment for Methanol Production and Co-Capture of Carbon Dioxide by Pressure Swing Adsorption. *Separation Science and Technology*, 47(6):850–866, 2012.

[50] S. Samadi, S. Lechtenböhmer, C. Schneider, K. Arnold, M. Fischedick, D. Schüwer, and A. & Pastowski. Decarbonization pathways for the industrial cluster of the Port of Rotterdam. Technical report, Wuppertal, 2017.

[51] C. Schneider, S. Lechtenböhmer, and S. Samadi. Risks and opportunities associated with decarbonising Rotterdam's industrial cluster. *Environmental Innovation and Societal Transitions*, 35(June 2019):414–428, 2020.

[52] SenterNovem. The Netherlands: list of fuels and standard CO2 emission factors. https://www.rvo.nl/sites/default/files/2013/10/Vreuls%202005%20NL%20Energiedragerlijst%2 %20Update.pdf, 2004.

[53] M. Siedlecki, W. de Jong, and A.H.M. Verkooijen. Fluidized bed gasification as a mature and reliable technology for the production of bio-syngas and applied in the production of liquid transportation fuels-a review. *Energies*, 4(3):389–434, 2011.

[54] C. C. Sreejith, C. Muraleedharan, and P. Arun. Equilibrium modeling and regression analysis of biomass gasification. *Journal of Renewable and Sustainable Energy*, 4(6), 2012.

[55] C. C. Sreejith, C. Muraleedharan, and P. Arun. Performance prediction of steam gasification of wood using an ASPEN PLUS thermodynamic equilibrium model. *International Journal of Sustainable Energy*, 33(2):416–434, 2014.

[56] Statista. Price of natural gas for industry in the Netherlands from 2008 to 2019. https://www.statista.com/statistics/595650/natural-gas-price-netherlands/, 2020.

[57] Statista. Sugar cane production volume Colombia (2010 - 2019). https://www.statista.com/statistics/874073/sugarcane-production-volume-colombia/, 2020.

[58] M. Svanberg, J. Ellis, J. Lundgren, and I. Landälv. Renewable methanol as a fuel for the shipping industry. *Renewable and Sustainable Energy Reviews*, 94(March):1217–1228, 2018.

[59] The Ministry of Infrastructure and the Environment. White Paper on Offshore Wind Energy. page 72, 2014.

[60] TNO. Electric industrial boiler. *Technology Factsheet*, (Berenschot 2017):1–2, 2018.

[61] TNO. H2 INDUSTRIAL BOILER. *Technology Factsheet*, (2012), 2020.

[62] UNFCCC. Adoption of the Paris Agreement. Report No. FCCC/CP/2015/L.9/Rev.1. http://unfccc.int/resource/docs/2015/cop21/eng/l09r01.pdf, 2015.

[63] X. Wang and Z. Bie. An MILP-based optimal energy flow of regional multiple energy network. *IEEE*, (2017 IEEE Conference on Energy Internet and Energy System Integration (EI2)):1–6, 2017.

[64] L. Weimann, P. Gabrielli, Annika Boldrini, Gert Jan Kramer, and Matteo Gazzani. On the role of H2 storage and conversion for wind power production in the Netherlands. *Computer Aided Chemical Engineering*, 46(2018):1627–1632, 2019.

[65] L. Weimann, A. Grimm, J. Nienhuis, P. Gabrielli, G.J. Kramer, and M. Gazzani. Energy System Design for the Production of Synthetic Carbon-neutral Fuels from Air-captured CO2. *Computer Aided Chemical Engineering*, 48:1471–1476, 2020.

[66] H. Zhang, L. Wang, M. Pérez-Fortes, J. Van herle, F. Maréchal, and U. Desideri. Techno-economic optimization of biomass-to-methanol with solid-oxide electrolyzer. *Applied Energy*, 258(May 2019):114071, 2020.

[67] H. Zhang, L. Wang, J. van Herle, F. Maréchal, and U. Desideri. Techno-economic optimization of CO2-to-methanol with solid-oxide electrolyzer. *Energies*, 12(19), 2019.

[68] Y. Zhang, J. Xiao, and L. Shen. Simulation of methanol production from biomass gasification in interconnected fluidized beds. *Industrial and Engineering Chemistry Research*, 48(11):5351–5359, 2009.

8 Appendix

A1. Key performance indicators biomass gasification process

Table 10: Key performance indicators of the biomass gasification process using Colombian sugar cane bagasse as biomass type

Biomass type: Sugar cane bagasse					
Route: CO_2 utilisation route					
SBR	kWh electricity/kWh MeOH	kWh heat/kWh MeOH	kWh H_2/kWh MeOH	kg biomass/kWh MeOH	kg CO_2/kWh MeOH
0.3	0.118	0.102	0	0.384	0.182
0.53	0.118	0.170	0	0.365	0.187
0.76	0.118	0.234	0	0.349	0.192
1	0.119	0.297	0	0.337	0.197
Route: CO_2 emitting route					
0.3	0.099	0.102	0	0.384	0.182
0.53	0.099	0.170	0	0.365	0.187
0.76	0.099	0.234	0	0.349	0.192
1	0.099	0.297	0	0.337	0.197
Route: Hydrogen addition route					
0.3	0.095	0.055	0.408	0.209	0.007
0.53	0.095	0.098	0.386	0.209	0.016
0.76	0.095	0.141	0.362	0.211	0.025
1	0.095	0.189	0.334	0.215	0.035

Table 11: Key performance indicators of the biomass gasification process using Nordic wood residue as biomass type

Biomass type: Nordic wood residue					
Route: CO_2 utilisation route					
SBR	kWh electricity/kWh MeOH	kWh heat/kWh MeOH	kWh H_2/kWh MeOH	kg biomass/kWh MeOH	kg CO_2/kWh MeOH
0.3	0.126	0.097	0	0.366	0.147
0.53	0.126	0.162	0	0.348	0.152
0.76	0.127	0.223	0	0.333	0.157
1	0.127	0.283	0	0.321	0.162
Route: CO_2 emitting route					
0.3	0.111	0.097	0	0.366	0.147
0.53	0.111	0.162	0	0.348	0.152
0.76	0.111	0.223	0	0.333	0.157
1	0.111	0.283	0	0.321	0.162
Route: Hydrogen addition route					
0.3	0.107	0.060	0.352	0.225	0.000
0.53	0.107	0.097	0.366	0.208	0.000
0.76	0.107	0.130	0.377	0.194	0.001
1	0.107	0.172	0.352	0.197	0.009

Table 12: Key performance indicators of the biomass gasification process using Indonesian rice straw as biomass type

Biomass type: Indonesian Rice Straw

SBR	kWh electricity/kWh MeOH	kWh heat/kWh MeOH	kWh H_2/kWh MeOH	kg biomass/kWh MeOH	kg CO_2/kWh MeOH
Route: CO_2 utilisation route					
0.3	0.126	0.099	0	0.374	0.149
0.53	0.126	0.166	0	0.356	0.154
0.76	0.127	0.228	0	0.341	0.159
1	0.127	0.290	0	0.329	0.164
Route: CO_2 emitting route					
0.3	0.111	0.099	0	0.374	0.149
0.53	0.111	0.166	0	0.356	0.154
0.76	0.111	0.228	0	0.341	0.159
1	0.111	0.290	0	0.329	0.164
Route: Hydrogen addition route					
0.3	0.107	0.060	0.358	0.228	0.000
0.53	0.107	0.098	0.372	0.210	0.000
0.76	0.107	0.133	0.379	0.198	0.001
1	0.107	0.177	0.354	0.201	0.010

A2. Key performance indicators, constraints & cost parameters of auxiliary technologies

Table 13: Key performance indicators of auxiliary technologies, with α being the first order energetic efficiency, β the second order energetic efficiency, S_{min} the minimum size (in kW) and S_{max} the maximum size (in kW), η being the (dis)charge efficiency, t_{var} being the time variation, Θ the storage loss coefficient and τ the (dis)charging time. For the DAC unit, the conversion for electrical to thermal energy is given as a fixed number, while the electrical and thermal requirement are dependent on the relative humidity of the air (ϕ).

Performance indicators conversion technologies

Technology	α	β	S_{min}	S_{max}
Gas boiler	0.92	-	{20; 70; 200}	{70, 200, 2.5e6}
H_2 boiler	0.92	-	{20; 70; 200}	{70, 200, 2.5e6}
Electric boiler	0.99	-	{20; 70; 200}	{70, 200, 2.5e6}
PEMEC	{0.60, 0.55, 0.53, 0.51}	{-0.01, 0.02, 0.01, 0.03}	{0; 100; 400}	{100; 400; 1e6}
PEMFC	{0.59, 0.54, 0.50, 0.47}	{-0.01, 0.02, 0.06, 0.11}	{0; 100; 400}	{500; 1330; 1e6}

Performance indicators storage technologies

Technology	η	t_{var}	Θ	τ	S_{min}	S_{max}
Battery	0.93	0.001	0	3		
Hydrogen storage	1	0	0	4		

Performance indicators DAC unit

Technology	E_{el}	E_{th}	E_{el} to E_{th}	$Module_{min}$	$Module_{max}$
DAC	f(ϕ)	f(ϕ)	0.97	0	200000

Table 14: Cost parameters of auxiliary technologies with λ being the variable investment costs, μ the fixed investment costs and Ψ being the maintenance fraction in terms of the total annual investment costs

Cost indicators for the different conversion and storage technologies			
Technology	λ	μ	Ψ
Gas boiler	{194.1; 82.4; 65.2} EUR/kW	{0; 6.88; 10.4} $\cdot 10^3$	0.02
H_2 boiler	{194.1; 82.4; 65.2} EUR/kW	{0; 6.88; 10.4} $\cdot 10^3$	0.02
Electric boiler	{194.1; 82.4; 65.2} EUR/kW	{0; 6.88; 10.4} $\cdot 10^3$	0.02
PEMEC	{2693; 1727; 1354} EUR/kW	{0; 9.67; 24.6} $\cdot 10^4$	0.05
PEMFC	{2160; 1680; 1320} EUR/kW	{0; 3.2; 8.0} $\cdot 10^5$	0.08
Battery	50 EUR/kWh		0.04
HOS	{20.7; 13.6; 10.9} EUR/kWh	{0; 235; 9466}	0.03
DAC	45385 EUR/unit		0.02
PV	375 EUR/m^2		0.04
WT Onshore	2.1 - 4.95 M€ /unit		0.04
WT Offshore	12 - 17.1 M€ /unit		0.04
Offshore CO_2 sink	{0.2; 0.09; 0.02} € /tCO_2/h	{36.5; 42.33; 51.64} $\cdot 10^6$	0.02

A3. Technology sizing & output for the different types of biomass for the case including a carbon sink

Technology sizes with carbon sink

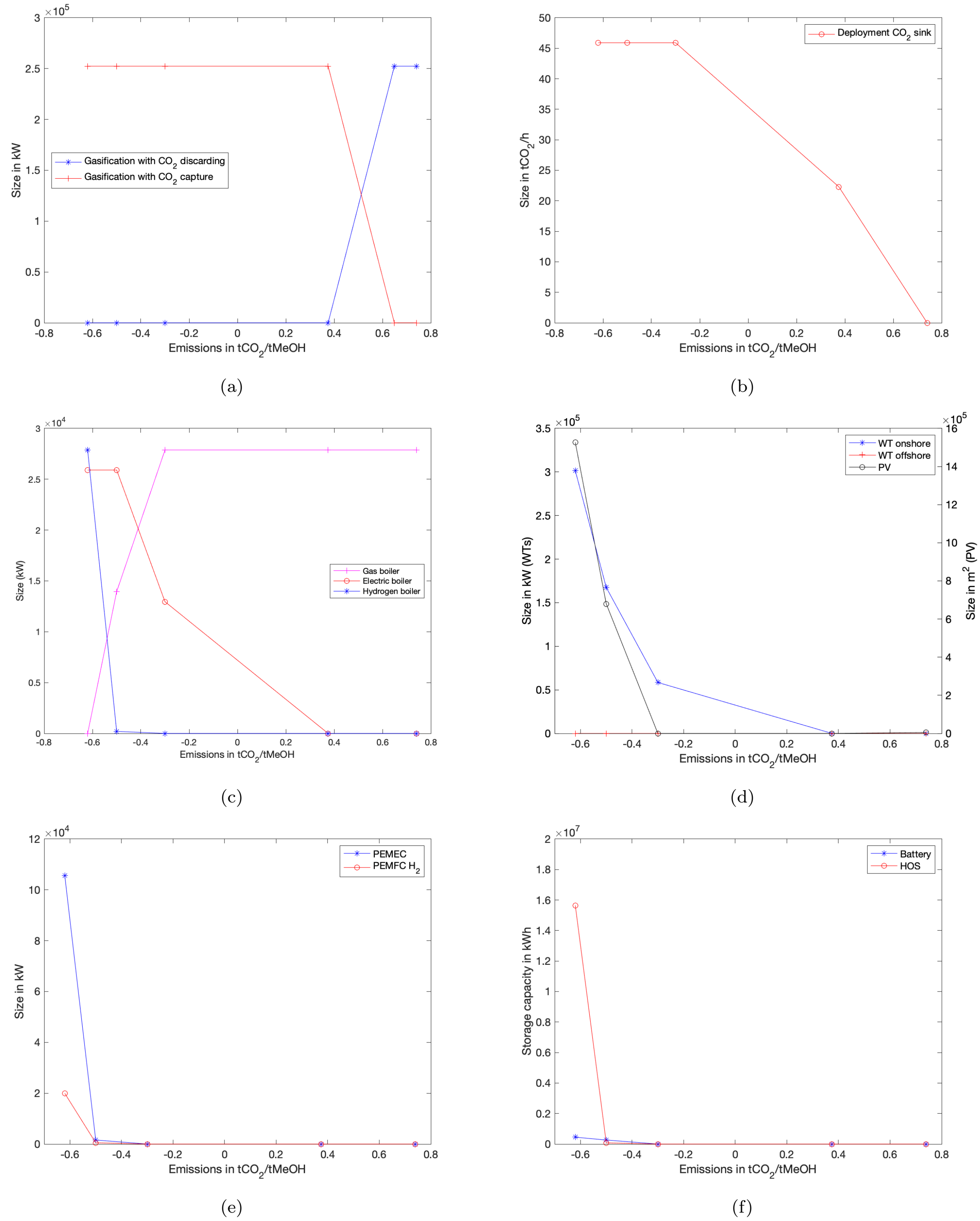

Figure 19: Technology sizes for the sugarcane bagasse case with (a) displaying the technology sizes of the methanol production units, (b) displaying the size of the carbon sink, (c) displaying the boiler sizes, (d) displaying the renewable energy technology sizes, (e) displaying the sizes of the hydrogen generating and consuming technologies and (f) displaying the sizes of the storage technologies

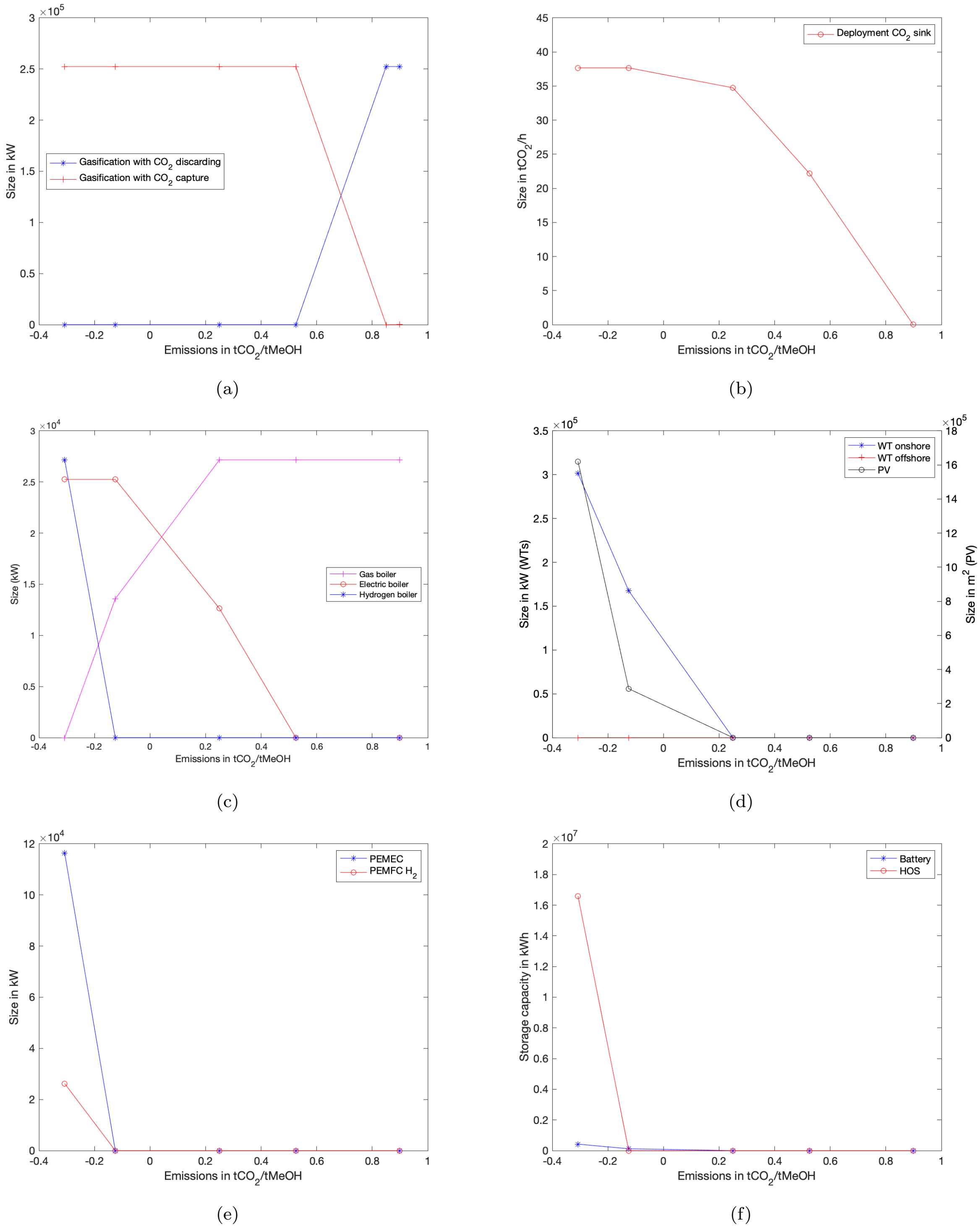

Figure 20: Technology sizes for the Indonesian rice straw case with (a) displaying the technology sizes of the methanol production units, (b) displaying the size of the carbon sink, (c) displaying the boiler sizes, (d) displaying the renewable energy technology sizes, (e) displaying the sizes of the hydrogen generating and consuming technologies and (f) displaying the sizes of the storage technologies

Technology output with carbon sink

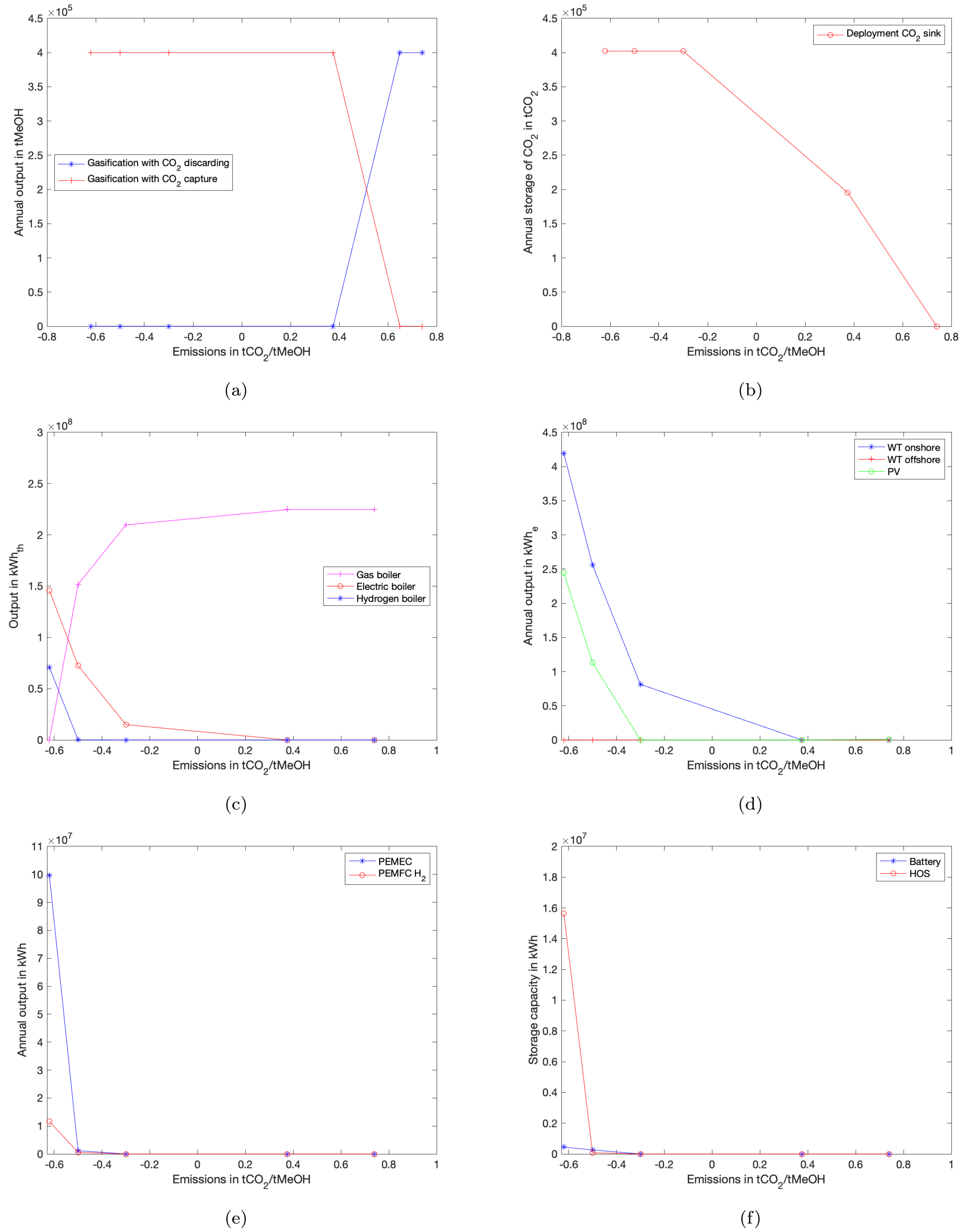

Figure 21: Annual technology outputs for the sugarcane bagasse case with (a) displaying the technology outputs of the methanol production units, (b) displaying the annual storage of CO_2 in the carbon sink, (c) displaying the boiler outputs, (d) displaying the renewable energy technology outputs, (e) displaying the outputs of the hydrogen generating and consuming technologies and (f) displaying the storage sizes of the storage technologies

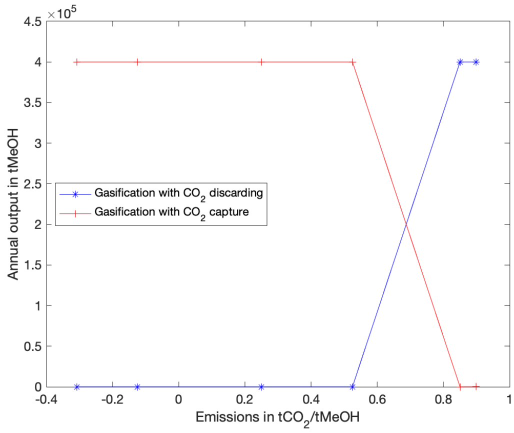

(a)

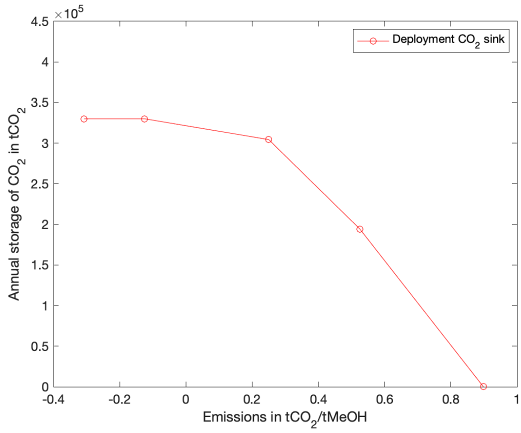

(b)

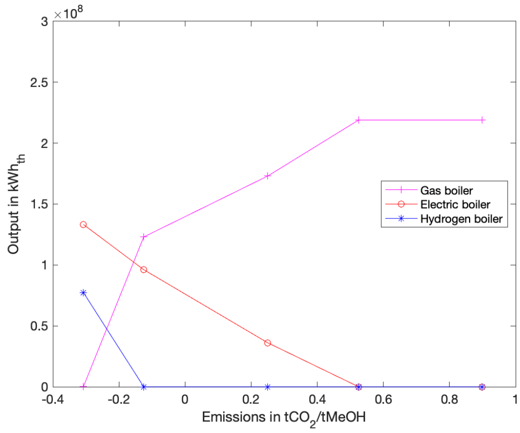

(c)

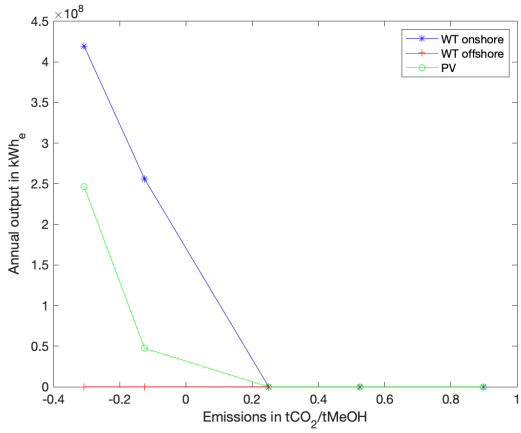

(d)

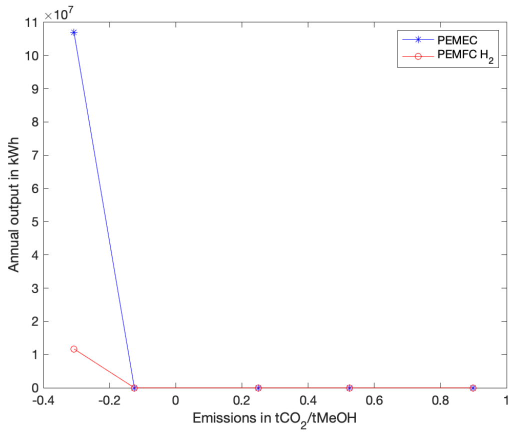

(e)

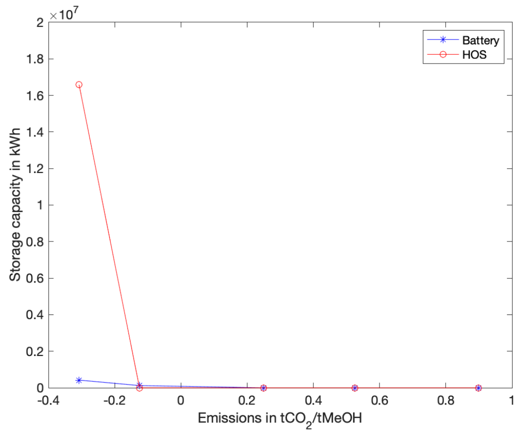

(f)

Figure 22: Annual technology outputs for the Indonesian rice straw case with (a) displaying the technology outputs of the methanol production units, (b) displaying the annual storage of CO_2 in the carbon sink, (c) displaying the boiler outputs, (d) displaying the renewable energy technology outputs, (e) displaying the outputs of the hydrogen generating and consuming technologies and (f) displaying the storage sizes of the storage technologies

A4. Technology sizing & output for the different types of biomass for the case excluding a carbon sink

Technology sizes without carbon sink

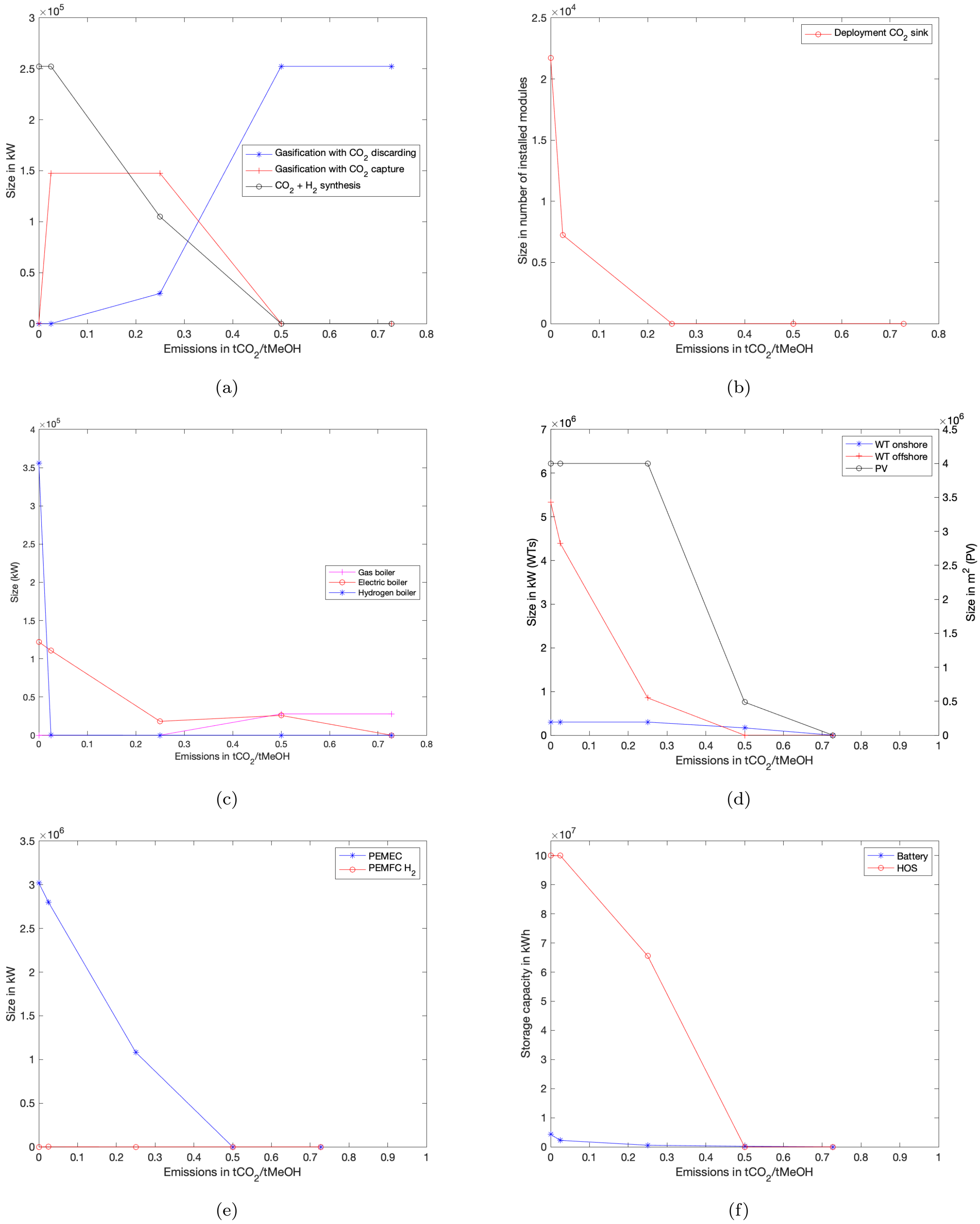

Figure 23: Technology sizes for the sugarcane bagasse case with (a) displaying the technology sizes of the methanol production units, (b) displaying the size of the DAC, (c) displaying the boiler sizes, (d) displaying the renewable energy technology sizes, (e) displaying the sizes of the hydrogen generating and consuming technologies and (f) displaying the sizes of the storage technologies

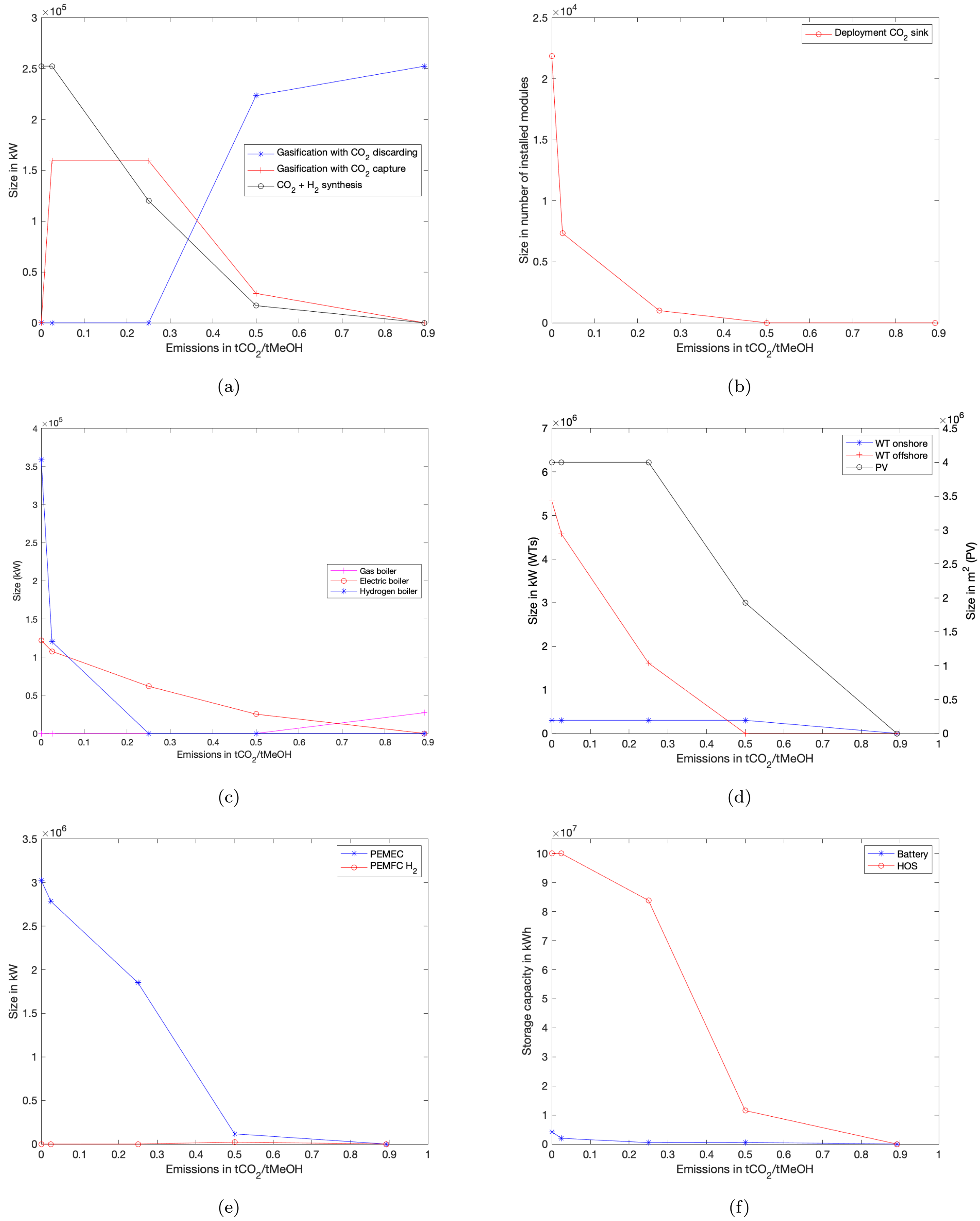

Figure 24: Technology sizes for the Indonesian rice straw case with (a) displaying the technology sizes of the methanol production units, (b) displaying the size of the DAC, (c) displaying the boiler sizes, (d) displaying the renewable energy technology sizes, (e) displaying the sizes of the hydrogen generating and consuming technologies and (f) displaying the sizes of the storage technologies

Technology output without carbon sink

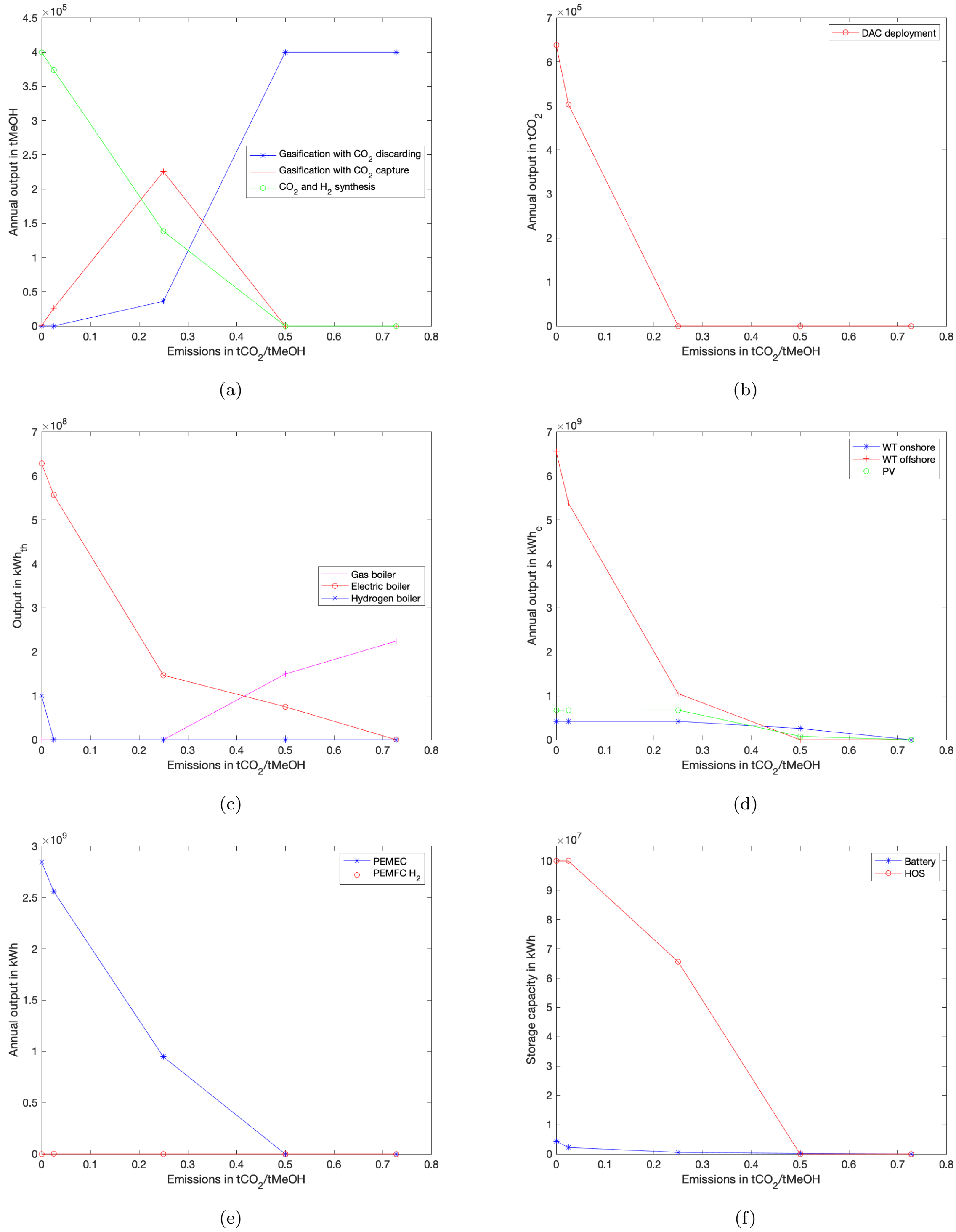

Figure 25: Annual technology outputs for the sugarcane bagasse case with (a) displaying the technology outputs of the methanol production units, (b) displaying the annual production of CO_2 in the DAC, (c) displaying the boiler outputs, (d) displaying the renewable energy technology outputs, (e) displaying the outputs of the hydrogen generating and consuming technologies and (f) displaying the storage sizes of the storage technologies

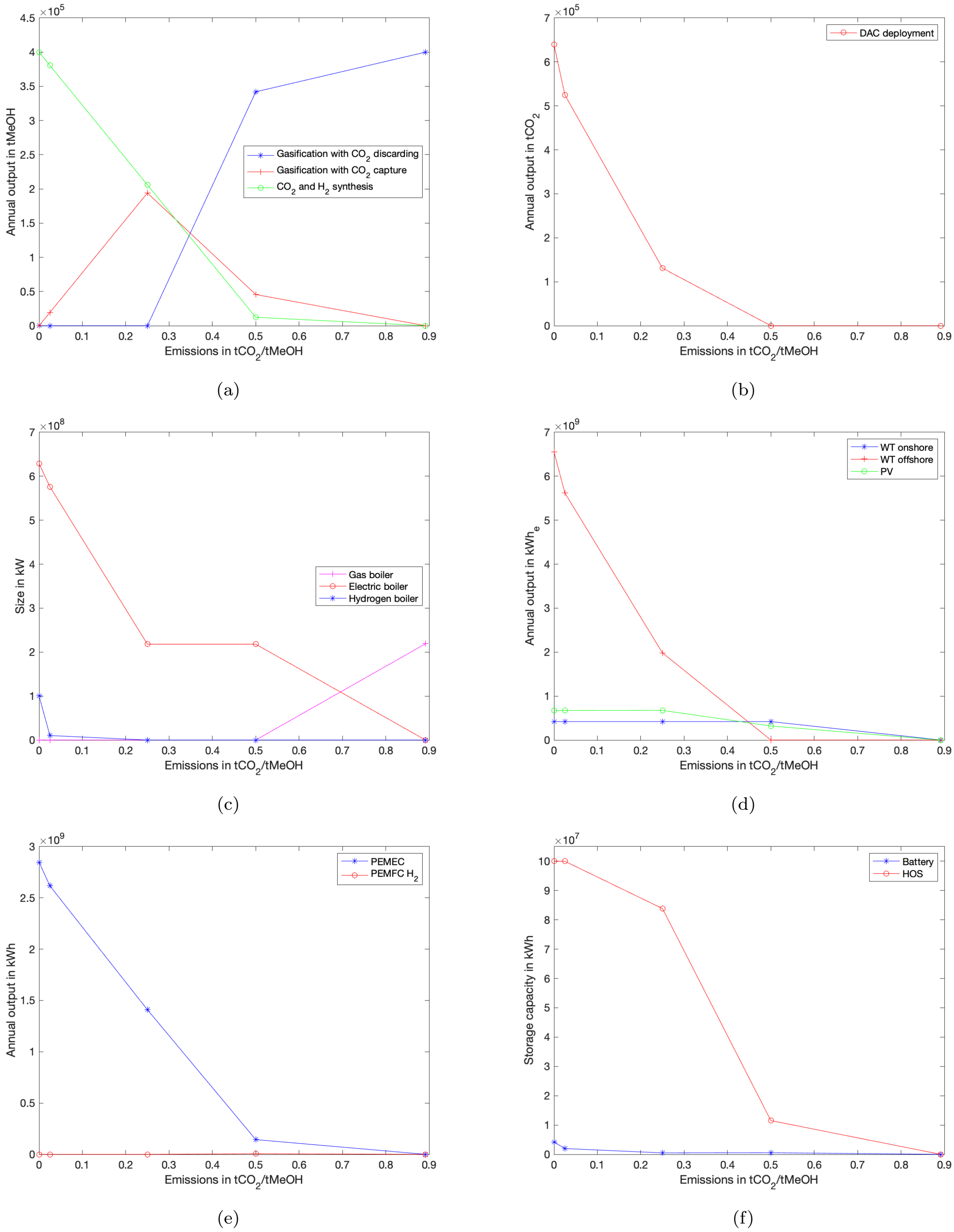

Figure 26: Annual technology outputs for the Indonesian rice straw case with (a) displaying the technology outputs of the methanol production units, (b) displaying the annual production of CO_2 in the DAC, (c) displaying the boiler outputs, (d) displaying the renewable energy technology outputs, (e) displaying the outputs of the hydrogen generating and consuming technologies and (f) displaying the storage sizes of the storage technologies